

AD-A148 290

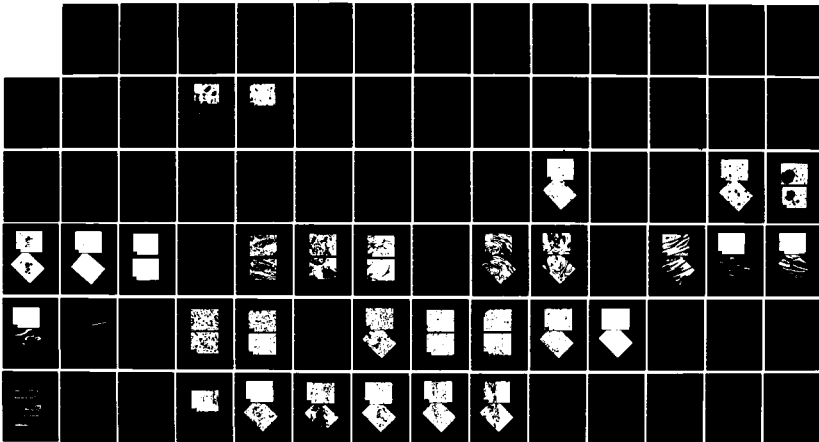
DISCLINATIONS IN CARBON-CARBON COMPOSITES(U) ACUREX
CORP/AEROTHERM MOUNTAIN VIEW CA J E ZIMMER ET AL.
SEP 84 TR-84-17/ATD N00014-81-C-0641

1/1

UNCLASSIFIED

F/G 11/4

NL

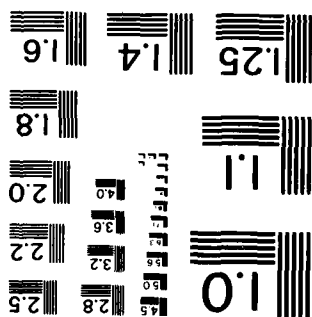


END

F/G 11/4

NL

MICROCOPY RESOLUTION TEST CHART
NATIONAL BUREAU OF STANDARDS-1963-A



Acurex Technical Report TR-84-001A

DISCLINATIONS IN CARBON-CARBON COMPOSITES

September 1984

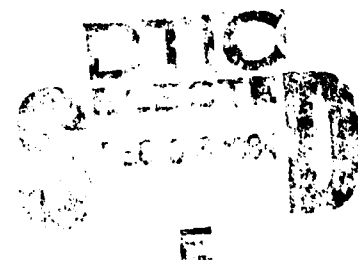
Interim Technical Report
July 1983 - July 1984
Contract N00014-81-C 0641

For

Office of Naval Research
800 North Quincy Street
Arlington, Virginia 22217

By

J.E. Zimmer and R.L. Weitz
Acurex Corporation
Aerotherm Division
555 Clyde Avenue
P.O. Box 7555
Mountain View, California 94039



84 11 08 084

SECURITY CLASSIFICATION OF THIS PAGE (When Data Entered)

DD FORM 1473 • EDITION OF 1 NOV 68 IS OBSOLETE

SECURITY CLASSIFICATION OF THIS PAGE (When Data Entered)

UNCLASSIFIED

SECURITY CLASSIFICATION OF THIS PAGE (When Data Entered)

Samples of A240 petroleum pitch, and graphite-fiber bundles and fabric impregnated with the pitch, were pyrolyzed by radiant heating in the presence of a magnetic field of 5500G.

The disklike molecules of the mesophase are aligned parallel to the magnetic field with the normals to the molecules lying anywhere in the plane perpendicular to the magnetic field. In the magnetic field, the spherules, which first form during the mesophase transformation from pitch, are aligned with their polar axes in this plane perpendicular to the magnetic field. The bulk mesophase (coalesced spherules) is oriented by the magnetic field to the fibrous microstructure with all the molecular layers lying parallel to the magnetic field and thus all the wedge disclinations aligned parallel to the magnetic field.

The magnetic field did not have a significant effect on the alignment of the mesophase within a graphite-fiber bundle. The strong anchoring forces which align the disklike molecules parallel to the filament surfaces could not be overcome by the magnetic field. The distance over which the competing effects of anchoring and magnetic field act is the magnetic coherence length. Measurement of the length led to calculation, for the first time, of the elastic constant describing the bend curvature of the molecular layers. This bend elastic constant is about 10^{-5} dynes, which is about ten times larger than the constant for conventional rodlike liquid crystals.

The pyrolysis of a bidirectional fiber composite in the presence of the magnetic field has shown that the matrix between the fiber bundles can be oriented perpendicular to the graphite-fiber fabric plies when the magnetic field direction is perpendicular to the fabric plies. This oriented matrix should provide improved resistance to interlaminar shear fracture.

FOREWORD

This is the third annual report on a program to study the disclinations in carbon-carbon composites. The work is supported by the Office of Naval Research under Contract N00014-81-C-0641. Dr. L. H. Peebles, Jr. is the Scientific Officer; his interest and support are gratefully acknowledged.

Accession For	
NTIS GRA&I	<input checked="checked" type="checkbox"/>
DTIC TAB	<input type="checkbox"/>
Unannounced	<input type="checkbox"/>
Justification	
By	
Distribution/	
Availability Codes	
Dist	Avail and/or Special
A-1	



TABLE OF CONTENTS

	<u>Page</u>
INTRODUCTION	1
BACKGROUND	3
Disclinations in a Fiber Bundle	7
Molecular Diamagnetism	10
Orientation of Mesophase by Magnetic Field	12
EXPERIMENTAL PROCEDURE	21
RESULTS	27
Alignment of Mesophase Spherules	27
Alignment of Bulk Mesophase	36
Alignment of Mesophase in Fiber Bundle	43
Magnetic Coherence Length and Bend Elastic Constant	58
Alignment in Fiber Composite	60
PUBLICATION	71
REFERENCES	75

LIST OF ILLUSTRATIONS

<u>Figure</u>		<u>Page</u>
1	Schematic model of the carbonaceous mesophase, a discotic nematic liquid crystal	4
2	Wedge disclinations in the carbonaceous mesophase	5
3	Twist disclinations in the carbonaceous mesophase	5
4	Reflectance of polarized light from a graphite crystal	6
5	Micrograph and structural sketch of matrix among graphite filaments in fiber bundle	8
6	Micrograph and structural sketch of disclinations in the matrix in a fiber bundle with an S = -2 disclination in a hexagonal array	9
7	Schematic diagram of fracturing in graphite-fiber bundle	11
8	Anisotropic diamagnetism of an aromatic ring	13
9	Formula for rodlike nematogenic molecules PAA and MBBA	14
10	Two hypothetical structures for the average molecule in the carbonaceous mesophase	14
11	Alignment of aromatic molecules by magnetic field	15
12	Schematic drawing of mesophase spherules in a uniform magnetic field: (a) static sample, (b) sample rotated about z-axis	17
13	Chemical formula of the hexaalkoxybenzoates of triphenylene	19
14	Experimental setup for pyrolysis in magnetic field	22
15	Wiring diagram	23
16	Sectioning plan	25
17	Optical micrographs of mesophase spherules aligned by magnetic field: 2000G, A240 pitch, 440°C	28
18	Extinction-contour patterns for Brooks-and-Taylor spherules oriented in a magnetic field	30

LIST OF ILLUSTRATIONS (Continued)

<u>Figure</u>		<u>Page</u>
19	Optical micrographs of mesophase spherules aligned by magnetic field: 2000G, A240 pitch, 440°C	31
20	Micrograph of spherules aligned in magnetic field	32
21	Micrographs of mesophase spherules formed in the absence of the magnetic field: A240 pitch, 440°C	33
22	Spherules formed in the absence of the magnetic field	34
23	Single orientation of mesophase spherules from rotation of sample in magnetic field: A240 pitch, 420°C	35
24	Optical micrograph of bulk mesophase: 2000G, A240 pitch, 440°C	37
25	Micrograph of bulk mesophase in 2000G magnetic field	38
26	Micrographs of bulk mesophase rotated in magnetic field: 2000G, A240 pitch, 500°C	39
27	Optical micrographs of bulk mesophase aligned by magnetic field: 5500G, A240 pitch, 460°C, section perpendicular to field	41
28	Micrographs of aligned bulk mesophase	42
29	Micrographs of aligned bulk mesophase	44
30	Micrographs of bulk mesophase aligned by magnetic field: 5500G, A240 pitch, 460°C, section parallel to field	45
31	Micrographs of aligned bulk mesophase	46
32	Micrographs of aligned bulk mesophase	47
33	Schematic diagram of fibrous structure of bulk mesophase aligned by a magnetic field	48
34	Micrographs of T300 fiber bundle parallel to magnetic field: 5500G, A240 pitch, 460°C	50
35	Micrographs of fiber bundle perpendicular to magnetic field	51

LIST OF ILLUSTRATIONS (Concluded)

<u>Figure</u>		<u>Page</u>
36	Micrographs of fiber bundle perpendicular to magnetic field	53
37	Micrographs of HM fiber bundle rotated in magnetic field perpendicular to the axis of rotation	54
38	Micrographs of fiber bundle rotated in magnetic field perpendicular to bundle axis	55
39	Micrographs of rotated fiber bundle showing alignment of bulk mesophase perpendicular to axis	56
40	Circular sheath about individual filament with bulk mesophase perpendicular to filament	57
41	Orientation of molecules anchored at filament surface and oriented by magnetic field	59
42	Optical micrographs of shear cracks in two-directional carbon-carbon composite	61
43	Schematic illustration of orientation of magnetic field and bidirectional composite	63
44	Structure of bidirectional composite; brightfield micrograph	64
45	Optical micrographs of fiber composite pyrolyzed in magnetic field perpendicular to fabric plies: 5500 gauss, A240 pitch, 460°C, cross-polarized light micrographs	65
46	Micrographs of bidirectional composite perpendicular to magnetic field	66
47	Micrographs of bidirectional composite perpendicular to magnetic field	67
48	Micrographs of bidirectional composite parallel to magnetic field	68
49	Micrographs of bidirectional composite parallel to magnetic field	69

INTRODUCTION

Disclinations are prominent in the microstructure of carbon-carbon composites, the principal material for thermal protection systems, such as rocket nozzles and reentry vehicle nosetips, and for high-temperature, structural components for turbine engines and tactical missiles. Disclinations are rotational elastic distortions in the graphite matrix of these composites introduced when the matrix was formed via the carbonaceous mesophase, a discotic nematic liquid crystal. The association of disclinations with the microstructure of carbon-carbon composites implies a relationship between the disclinations and the structure-sensitive physical properties of these composites. Thus, basic research is needed to not only understand the topological aspects of disclinations, but also to understand the disclination structures in carbon-carbon composites and the role of these disclinations in controlling the physical properties of these composites.

Carbon-carbon composites have graphitic matrices reinforced with high-strength, high-modulus graphite fibers from rayon, polyacrylonitrile or mesophase pitch. These composites exhibit some unique properties: their elastic modulus at room temperature is retained at elevated temperatures, their volumetric thermal expansion is quite low, and they have good fracture toughness. These properties exceed those of other ceramic materials with crystal lattices that do not contain disclinations. Disclinations are inherent in the carbon-carbon composites, since their microstructure is formed

during the transformation by pyrolysis of the matrix precursors such as petroleum and coal-tar pitches to the carbonaceous mesophase. Disclinations can exist in this liquid crystal because the high rotational strains of the disclinations are reduced by flow of the oriented molecules of the liquid crystal.

The objectives of this basic research on the disclinations in carbon-carbon composites are to identify and classify the disclination structures in the matrix of carbon-carbon composites and to determine the relationship of the disclinations to the fracture behavior of the composite matrix.

The specific area of research described in this report involves the study of the effect of a magnetic field on the alignment of the carbonaceous mesophase by itself as matrix between fiber bundles, within a fiber bundle, and within a bidirectional fiber composite. The objective of this research on the magnetic field effects was to determine how the disclination structures could be controlled or altered to improve the properties of the resulting carbon-carbon composite. For example, a weakness of two-directional carbon-carbon composites is easy delamination between adjacent fabric plies. Carbonization in a magnetic field perpendicular to the plies would tend to orient wedge disclinations perpendicular to the fabric plies. The plane of delamination would then be perpendicular to the wedge disclinations which would present a difficult fracture path for the delamination.

BACKGROUND

The carbonaceous mesophase is a unique liquid crystal formed during the pyrolysis of those organic materials that yield graphitizable cokes or chars.^{1,2} In the temperature range of 400° to 500°C, polymerization reactions occur to build large, disklike, polynuclear aromatic molecules, that, upon reaching molecular weights in the neighborhood of 1400, condense in parallel arrays and precipitate from the molten pitch as a liquid crystal, the carbonaceous mesophase. Initially, this mesophase forms as small spherules of simple structure, but, after coalescence to viscous bulk mesophase, quite complex morphologies are developed and eventually frozen-in as the pyrolyzing mass hardens to a coke. The carbonaceous mesophase has the structural characteristics of a discotic nematic liquid crystal -- an array of disklike molecules that tend to lie parallel to each other and display long-range orientational order, but are not required to be in point-to-point registry to adjacent molecules.³ This liquid crystal is shown schematically in Figure 1. Several possible molecular models are shown, based on the analysis of the mesophase by infrared spectroscopy, nuclear magnetic resonance spectroscopy, and vapor pressure osmometry.⁴

In the liquid crystal stage of pyrolysis, the basic morphologies of graphitic materials are established through spherule coalescence and deformation of the mesophase. These complex lamelliform morphologies necessarily contain structural discontinuities, that is, disclinations, in the

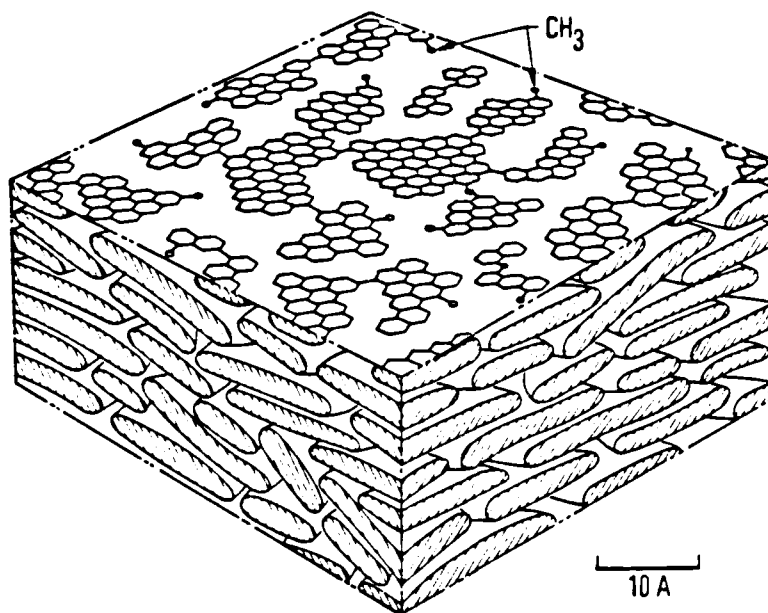


Figure 1. Schematic model of the carbonaceous mesophase, a discotic nematic liquid crystal

parallel stacking of the aromatic molecules.⁵ On a local scale, the parallel stacking in the mesophase is retained throughout a region of material. However, the orientation of the stacking changes continuously as the molecule layers bend, splay and twist, and map out singly and doubly curved surfaces. Topologically, space cannot be filled completely by these curved regions of stacked molecules and thus disclinations exist as the discontinuities in this complex morphology. The disclinations are characterized by a rotation vector of multiples of π , as described the the twofold symmetry of the discotic nematic liquid crystal. For the wedge disclinations of Figure 2, the rotation vector is parallel to the tangent to the disclination line (core), and for the twist disclinations of Figure 3, the rotation vector is perpendicular to the tangent.

The presence and types of disclinations is efficiently determined by reflection microscopy with polarized light. The preferred orientation of the

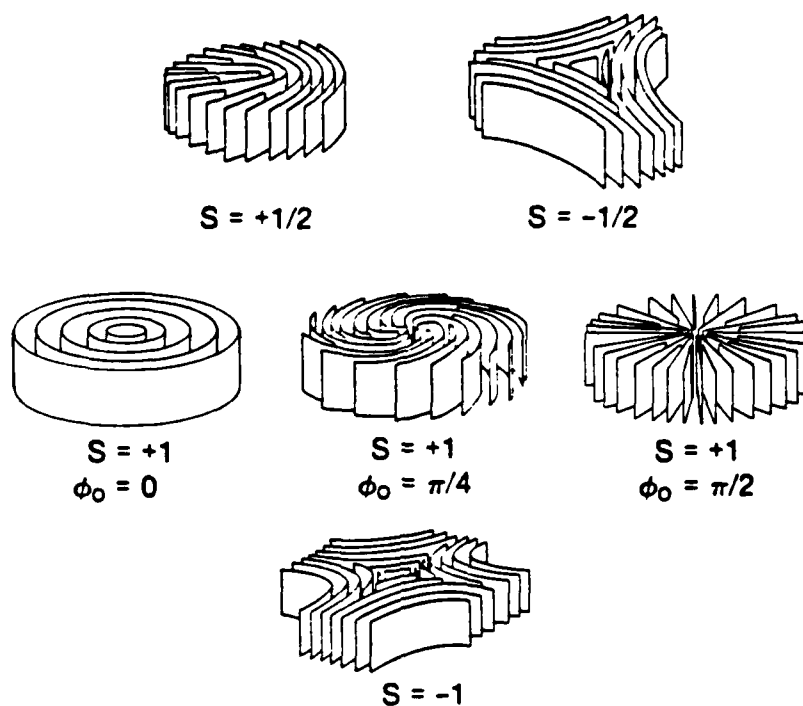


Figure 2. Wedge disclinations in the carbonaceous mesophase. The surfaces denote the layers mapped out by the average direction of the preferred orientation of the individual disklike molecules. The rotation vector is parallel to the tangent to the disclination line.

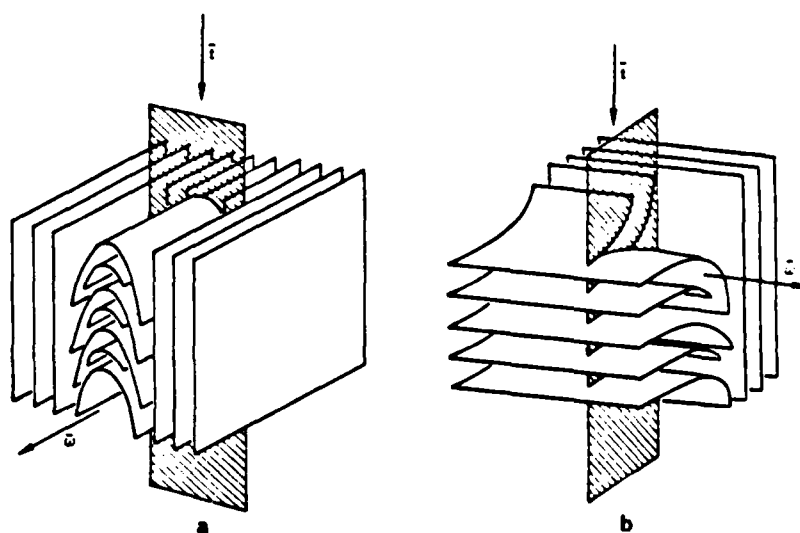


Figure 3. Twist disclinations in the carbonaceous mesophase. The rotation vector is perpendicular to the ribbonlike core.

mesophase as it intersects a polished plane of section can be defined with cross-polarized light. Crystalline graphite is birefringent (optically anisotropic) and thus the reflection of polarized light is dependent on its orientation to the preferred orientation of the mesophase. The reflection contrasts for a graphite single crystal are illustrated in Figure 4. With polarized-light micrography, disclinations are evident as rotation-invariant points in the extinction contours that identify mesophase layers that are perpendicular to a polarizing direction. The disclinations of strength $\pm 1/2$ are denoted by a node with two extinction-contour arms. For a rotation of the crossed polarizers, the arms of the $S = +1/2$ node rotate with the polarizers and the arms of the $S = -1/2$ node rotate counter to the polarizers. The disclinations of strength $S = \pm 1$ are denoted by a cross in the extinction contours -- a point with four extinction-contour arms. The $S = +1$ disclination is a corotating cross; the $S = -1$ disclination is a counterrotating cross. The polarized-light micrography at various angles of rotation of the polarizers is used to define the molecular orientations about these nodes and crosses in the extinction contours and thus map out the configurations of the underlying disclinations.²

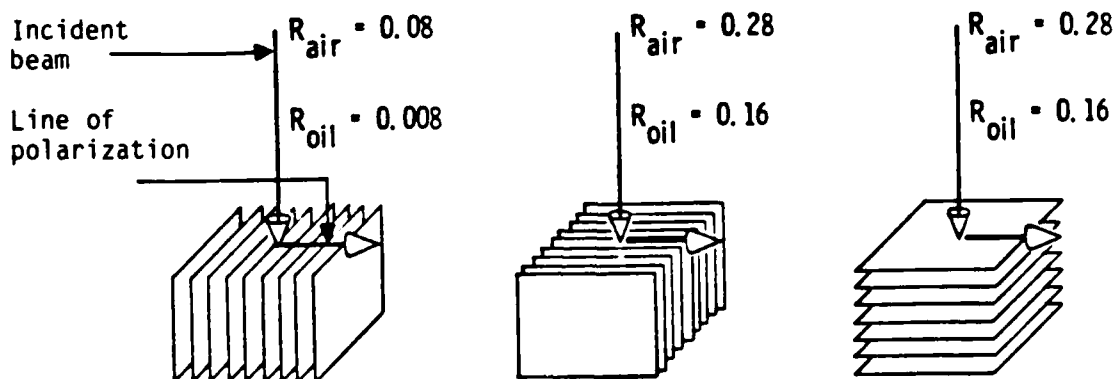


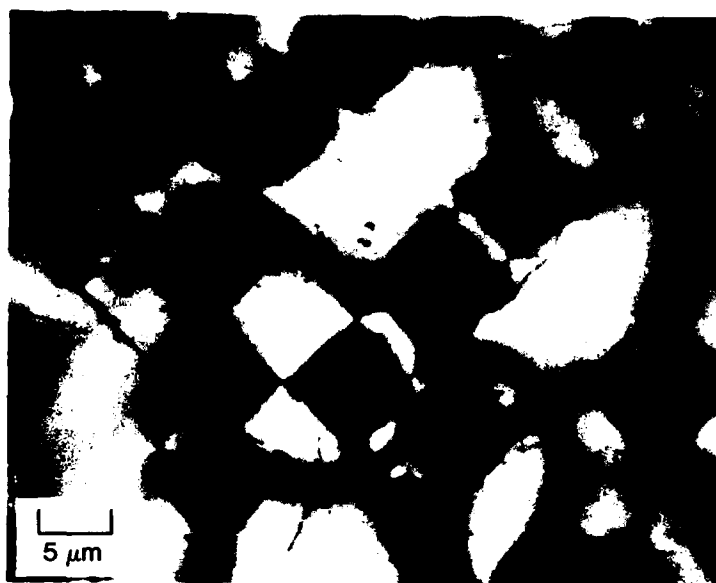
Figure 4. Reflectance of polarized light from a graphite crystal. The differences in reflectance for the carbonaceous mesophase are slightly smaller, but significant to delineate the disclination structures.

The complex, heterogeneous structure of multidirectional carbon-carbon composites consists of fiber bundles and matrix pockets, each with their own distinct microstructures. Disclinations exist in the matrix within the graphite-fiber bundles and in the matrix regions between fiber bundles. Each has its characteristic disclination structure and thus may play a different role in the relation of disclinations to the properties of the carbon-carbon composites.

Disclinations in a Fiber Bundle

In a carbon-carbon composite, the graphite filaments are typically aligned parallel as fiber bundles consisting of thousands of the filaments which are about 7 μm in diameter. Among these graphite filaments from rayon, polyacrylonitrile, or mesophase pitch is the graphite matrix formed via the carbonaceous mesophase. In this matrix, among the graphite filament are disclinations. The major aspects of the disclinations in a fiber bundle are the orientation of the filaments and the alignment of the mesophase by the filaments defines the type of disclination present, and the arrangement of the filaments prescribes the strength of the disclinations.

The disklike molecules of the carbonaceous mesophase prefer to align parallel to the surface of the graphite filaments. This tendency for the molecules of the mesophase to align parallel to substrate surfaces has been shown for graphite flakes, coke particles, and ceramic materials.^{6,7} The parallel alignment about the graphite filaments⁸ is shown in Figures 5 and 6. These micrographs show several of the round, graphite filaments and the surrounding matrix. The parallel alignment results in a circular sheath about each filament. This sheath is several microns in thickness and extends the length of each filament.



H-546

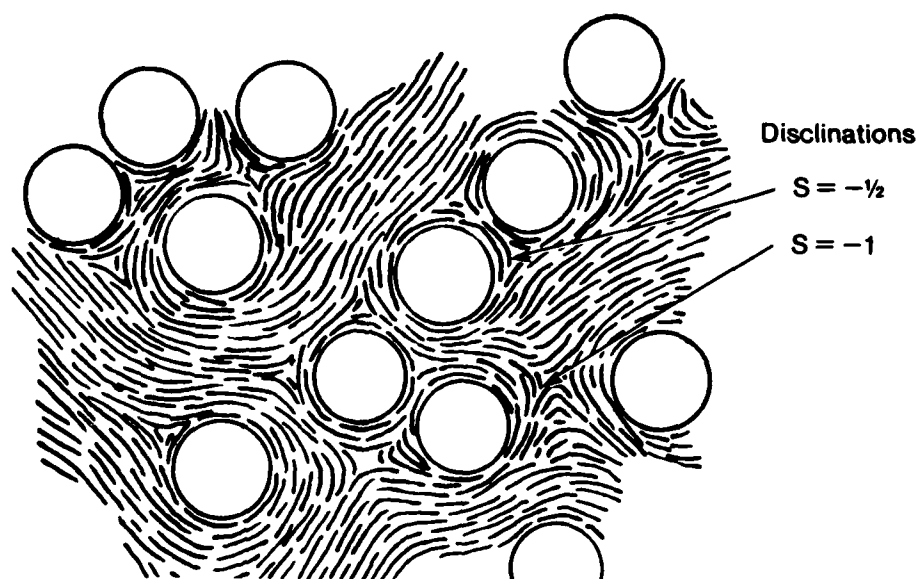
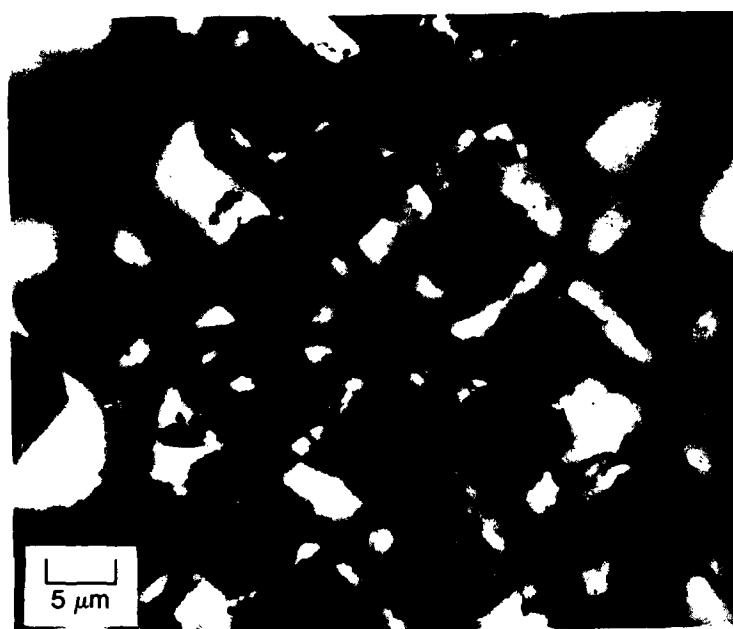


Figure 5. Micrograph and structural sketch of matrix among graphite filaments in fiber bundle. The mesophase aligns in a circular sheath about each filament.



H-545

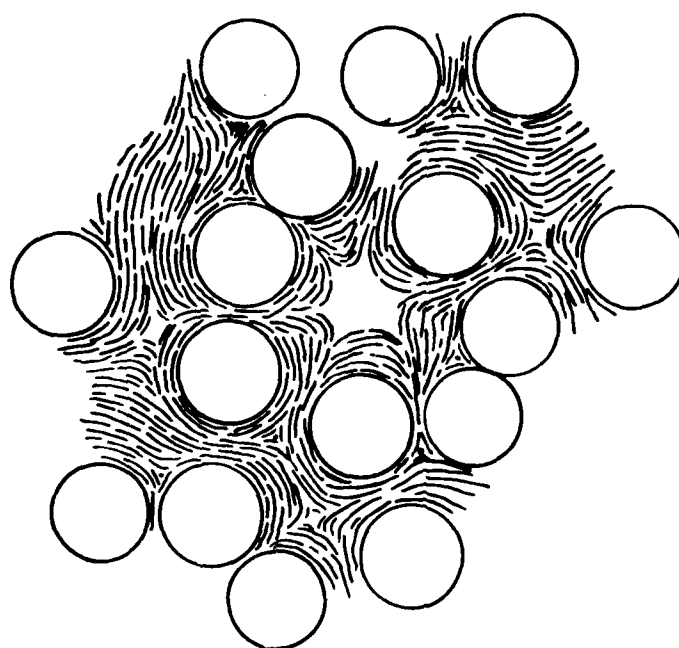


Figure 6. Micrograph and structural sketch of disclinations in the matrix in a fiber bundle with an $S = -2$ disclination in a hexagonal array.

Within a fiber bundle, the alignment of the mesophase as a circular sheath about the filaments prescribes the morphology of the remaining volume of matrix. Evident among the filaments are disclinations: those points where the parallel stacking of the mesophase layers is interrupted. These are wedge disclinations. The parallel alignment of the filaments and mesophase sheath force the disclination lines to be parallel to the filaments. The rotation vector for these disclinations is parallel to the disclination line and thus these disclinations are pure wedge disclinations.

The fracture behavior of these fiber bundles⁹ has shown that the crack path was controlled by the disclinations present and was diverted or altered depending on the type and structure of the disclinations. The disclinations produced a tongue-and-groove type of fracturing. The fracturing within a fiber bundle is shown schematically in Figure 7. The use of a magnetic field to orient the matrix about the filaments could offer a means for changing these fracture paths. Alignment of the molecular layers perpendicular to the filaments may promote a greater number of $S = -1$ disclinations with the saddlelike core. These $S = -1$ disclinations would force a more tortuous fracture path.

Molecular Diamagnetism

Most organic molecules are diamagnetic, the diamagnetism being particularly strong when the molecule is aromatic. In a diamagnetic material with zero net magnet moment in the absence of an applied field, a magnetic moment is induced opposite to an applied magnetic field. This is reverse from a paramagnetic material, in which the induced magnetic moment is parallel to the applied magnetic field. The magnetic susceptibility, a measure of the extent to which the material can be magnetized, is small and negative for a diamagnetic material. The susceptibility is small and positive for a

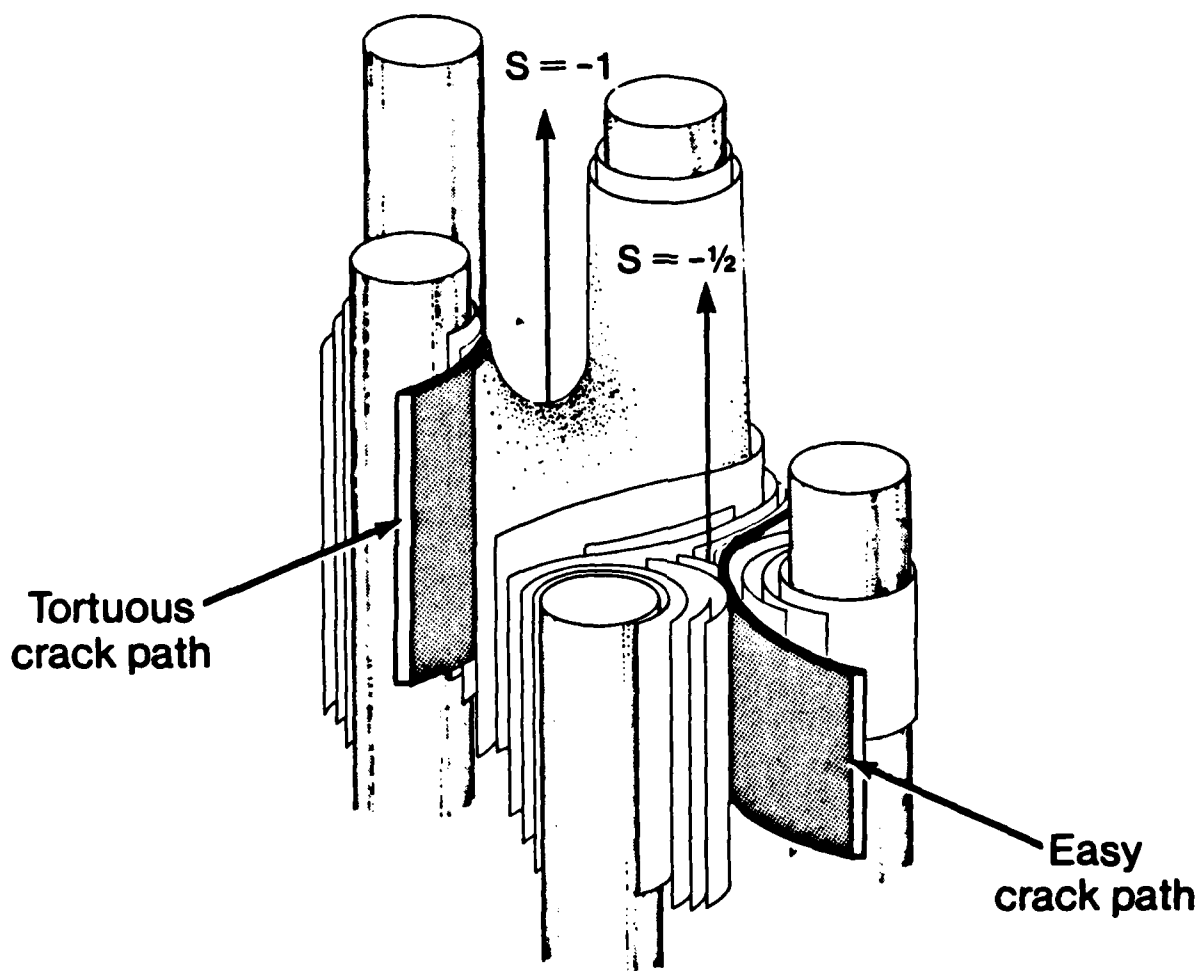


Figure 7. Schematic diagram of fracturing in graphite-fiber bundle

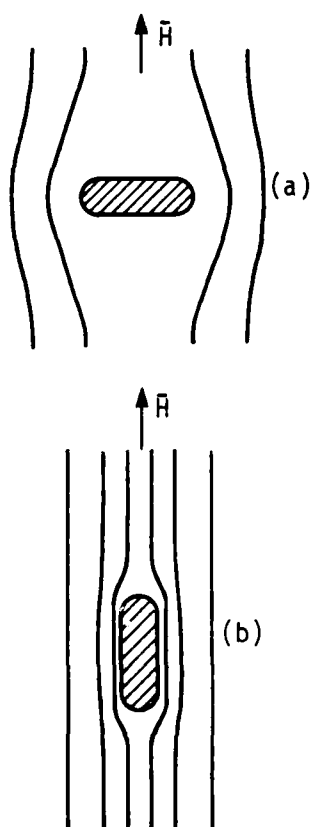
paramagnetic material. A benzene ring in a magnetic field H normal to its plane builds up a current inside the ring, which tends to reduce the flux going through it. Thus, the lines of force tend to be expelled, as shown in Figure 8. The energy is increased. If the field H is applied parallel to the ring, no current is induced, the lines of force are nearly undistorted, and the energy is not increased (Figure 8). Thus, an aromatic benzene molecule tends to orient such that the plane of the molecule is in the direction of the magnetic field.

Typical molecules of conventional nematic liquid crystals are rodlike in shape and contain several aromatic rings. For example, two classical nematogenic molecules, p-azoxyanisole (PAA) and N-(p-methoxybenzylidene)-p-butylaniline (MBBA) both have two benzene rings which are nearly coplanar (Figure 9). The lowest energy configuration is obtained when the optical axis (along the length of the molecule) is parallel to the applied magnetic field. This orientation is shown schematically in Figure 11.

The polynuclear aromatic molecules of the carbonaceous mesophase consist of several fused benzene rings giving the molecule a disklike shape (Figure 10). This aromatic molecule also is oriented by a magnetic field and tends to align parallel to the magnetic field as shown in Figure 11. However, the molecular orientation is not uniquely defined. With the use of the normal to the disklike molecule to define its orientation, the normals to the molecules in the magnetic field lie anywhere in the plane perpendicular to the magnetic field.

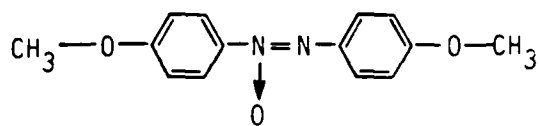
Orientation of Mesophase by Magnetic Field

Previous research on the effect of a magnetic field on the carbonaceous mesophase has centered on demonstration of the orientation of the mesophase by



ATD258-84

Figure 8. Anisotropic diamagnetism of an aromatic ring. (The ring is normal to the page.) In case (a), the lines of force are more distorted and the energy is higher.



ATD259-84

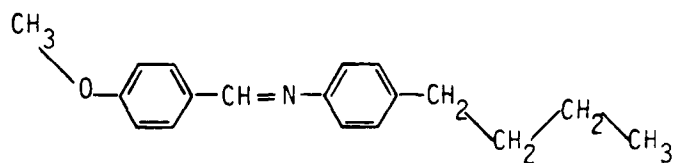
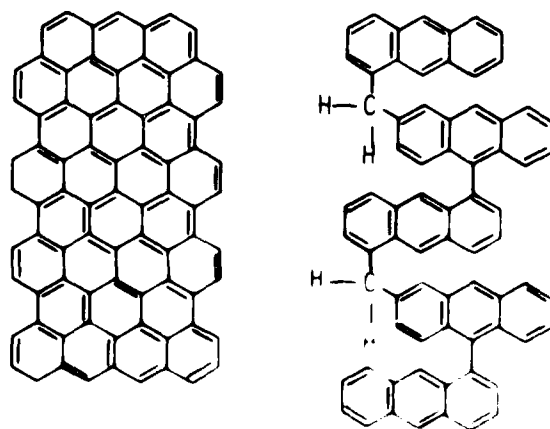
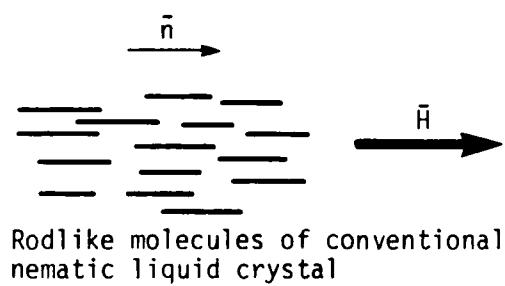


Figure 9. Formula for rodlike nematogenic molecules PAA (top) and MBBA



ATD260-84

Figure 10. Two hypothetical structures for the average molecule in the carbonaceous mesophase (after Dehaes, et al. [1])



ATD263-84

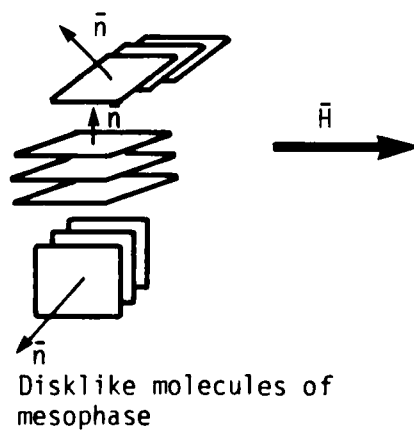
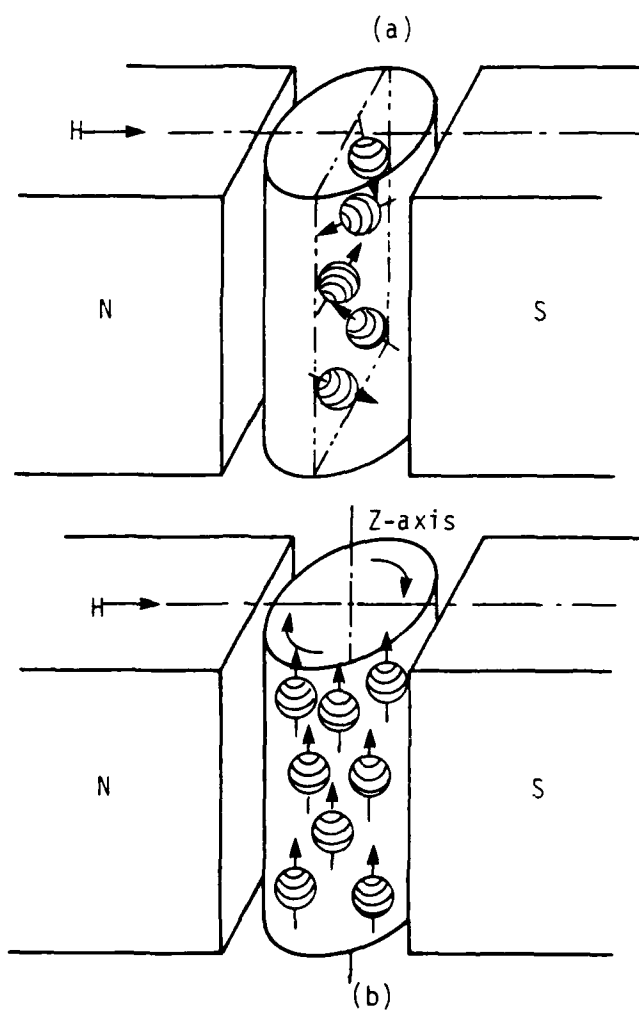
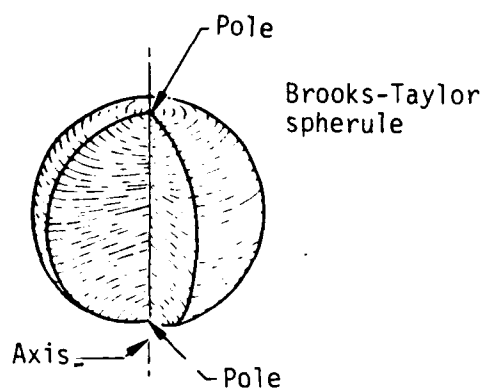


Figure 11. Alignment of aromatic molecules by magnetic field

a magnetic field and the use of a magnetic field for preparation of well-oriented samples for measurement of diamagnetic susceptibility. Initial work by Singer and Lewis¹⁰ showed that the spherules of the carbonaceous mesophase are oriented by a magnetic field. Samples of acenaphthylene pitch were heated in 5-mm OD Pyrex tubes at 430°C for 1 hr in a high-temperature cavity of an electron-spin-resonance apparatus. The sample weight was about 100 mg and the magnetic field strength was about 10 kG. Observation by optical microscopy of both the longitudinal (perpendicular to field) and transverse planes of section showed that the polar axes of the spherules all were aligned to lie in the plane perpendicular to the magnetic field, as shown in Figure 12. The aromatic molecules of the mesophase in a spherule align perpendicular to the polar axis. Thus, when the molecules align parallel to the field, the spherule axis is perpendicular to the field. A higher degree of orientation was obtained when the sample was rotated about an axis perpendicular to the magnetic field. The mesophase spherules were all oriented with their polar axes parallel to the axis of rotation, as shown in Figure 12. The rotation forces the aromatic molecules to lie in the plane of the magnetic field with the normal to the molecule parallel to the rotation axis. Thus, with both the magnetic field and sample rotation, the molecules of the mesophase are aligned in this unique orientation.

The diamagnetic susceptibility of the carbonaceous mesophase has been measured on a sample oriented by a magnetic field.¹¹ Mesophase pitch was prepared by heat treating a petroleum pitch. Small samples of the mesophase were heated to 400°C for 30 min in a magnetic field of about 10 kG. The resulting sample was essentially one large oriented mesophase domain with all the molecular layers perpendicular to the axis of rotation. Since the diamagnetism for the aromatic molecules is anisotropic, two susceptibilities



ATD261-84

Figure 12. Schematic drawing of mesophase spherules in a uniform magnetic field: (a) static sample, (b) sample rotated about z-axis

were measured. The quantities χ_{\perp} and χ_{\parallel} are the diamagnetic components measured with the magnetic field perpendicular and parallel, respectively, to the parallel orientation of the aromatic molecular layers. The diamagnetic susceptibilities of the carbonaceous mesophase are given here:

$$\chi_{\perp} = -1.19 \times 10^{-6} \text{ emu/g}$$

$$\chi_{\parallel} = -0.50 \times 10^{-6} \text{ emu/g}$$

and the diamagnetic anisotropy is

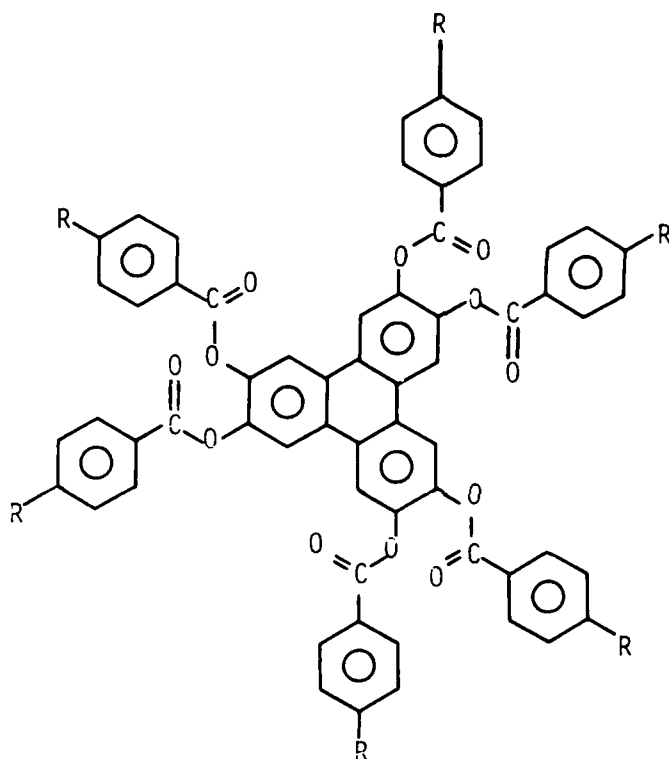
$$\chi_{\perp} - \chi_{\parallel} = -0.69 \times 10^{-6} \text{ emu/g} .$$

For comparison, the diamagnetic anisotropy has been measured for discotic nematic liquid crystals of pure molecules.¹² These are mesophases of the hexaalkoxybenzoates of triphenylene (Figure 13) where R is either an alkyl chain of six (C_6) or eleven (C_{11}) carbons. For these liquid crystals, the diamagnetic anisotropies are

$$C_6 \quad \chi_{\perp} - \chi_{\parallel} = -0.49 \times 10^{-7} \text{ emu/g}$$

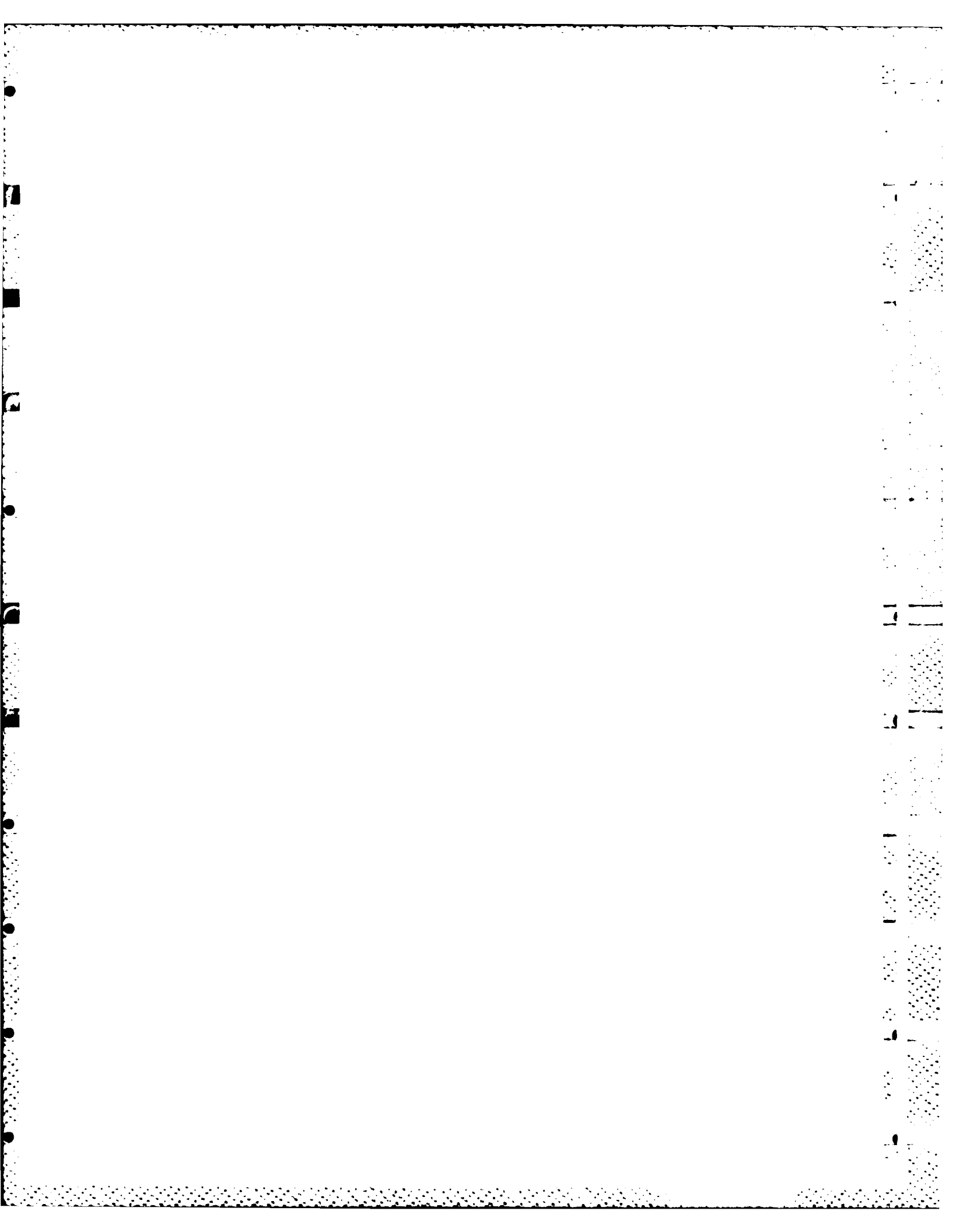
$$C_{11} \quad \chi_{\perp} - \chi_{\parallel} = -0.21 \times 10^{-7} \text{ emu/g} .$$

The difference between these values of diamagnetic anisotropy for the C_6 and C_{11} compounds results from a higher ratio of aromatic parts to aliphatic parts for the C_6 molecules; thus it has a larger anisotropy. Both the diamagnetic susceptibilities and the anisotropy of the carbonaceous mesophase are larger than those of the pure disklike mesophases. This indicates that the molecules of the carbonaceous mesophase have a much larger aromatic core.



ATD262-84

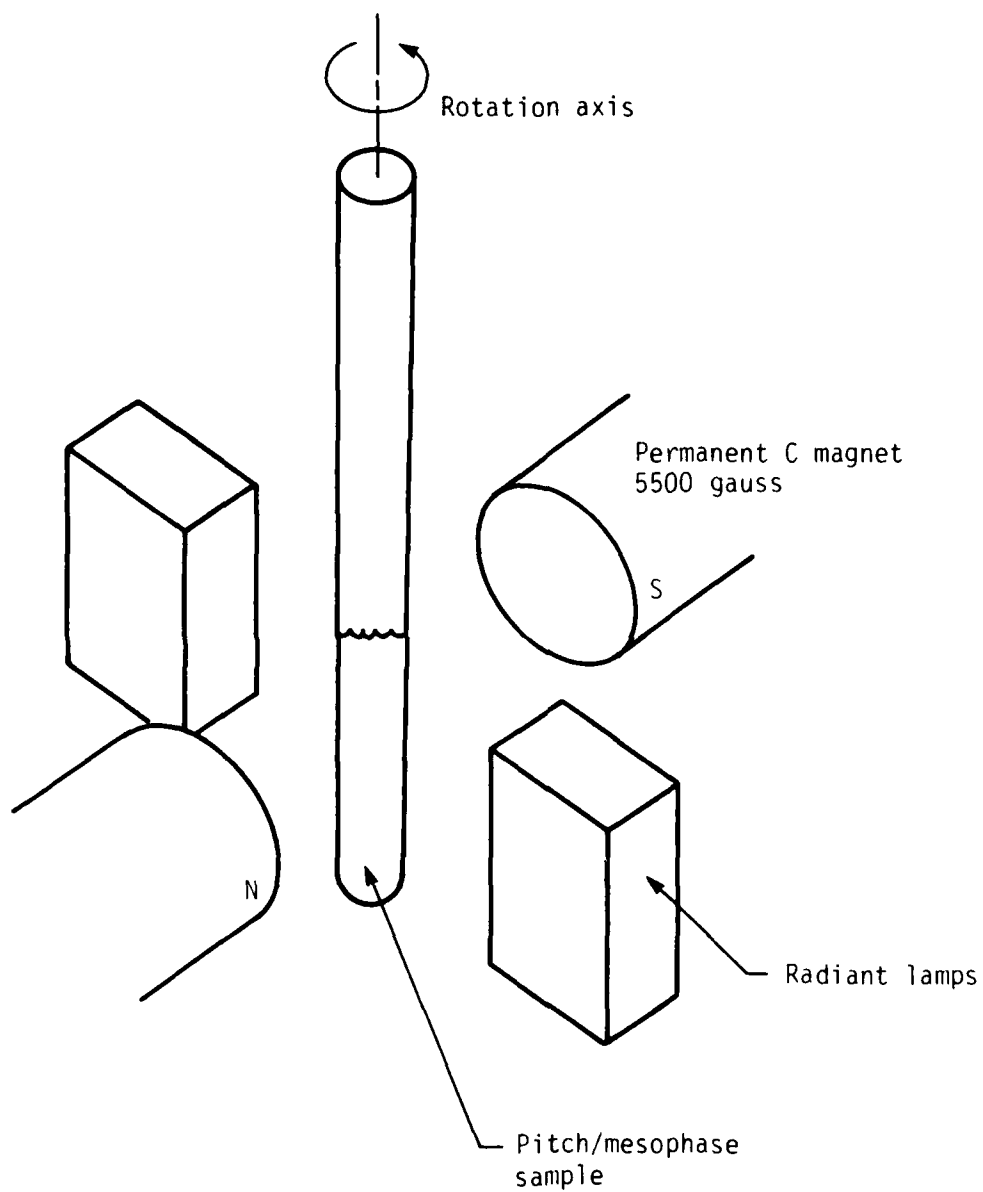
Figure 13. Chemical formula of the hexaalkoxybenzoates of triphenylene



EXPERIMENTAL PROCEDURE

The pyrolysis of a petroleum-pitch precursor and the transformation to the carbonaceous mesophase was conducted with the use of radiant lamps and in the presence of a magnetic field. The experimental setup is shown schematically in Figure 14. Glass test tubes of inside diameter of 10 mm were placed vertically between opposing radiant lamps. At 90° to the lamps were the poles of the permanent C magnet. The radiant lamps were used, rather than a resistively heated furnace, to eliminate any interference with the magnetic field. The effective heating area of the radiant lamps was 6.4 cm x 3.7 cm and the rated power was 0.5 kW. The lamps had a parabolic reflector surface. To ensure precise heating rates and temperature control, a phase-angle power controller was used in conjunction with a microprocessor temperature programmer (Figure 15). With the phase-angle power controller, the silicon-controlled rectifier (SCR) is fired late in each AC half-cycle to obtain constant output. A chromel-alumel thermocouple was placed in a graphite sleeve and inserted in the pitch. This radiant lamp-programmer system provided accurate temperature control to within $\pm 1^\circ\text{C}$.

Ashland A240 petroleum pitch was used as it is relatively free of inert quinoline insolubles which could interfere with the development of the mesophase structure. Approximately 1g of pitch was used in each test tube. The pyrolysis heating rate was 100°C/hr from room temperature to 380°C and 20°C/hr from 380°C to the desired temperature. The pyrolysis in the test tubes



ATD271-84

Figure 14. Experimental setup for pyrolysis in magnetic field

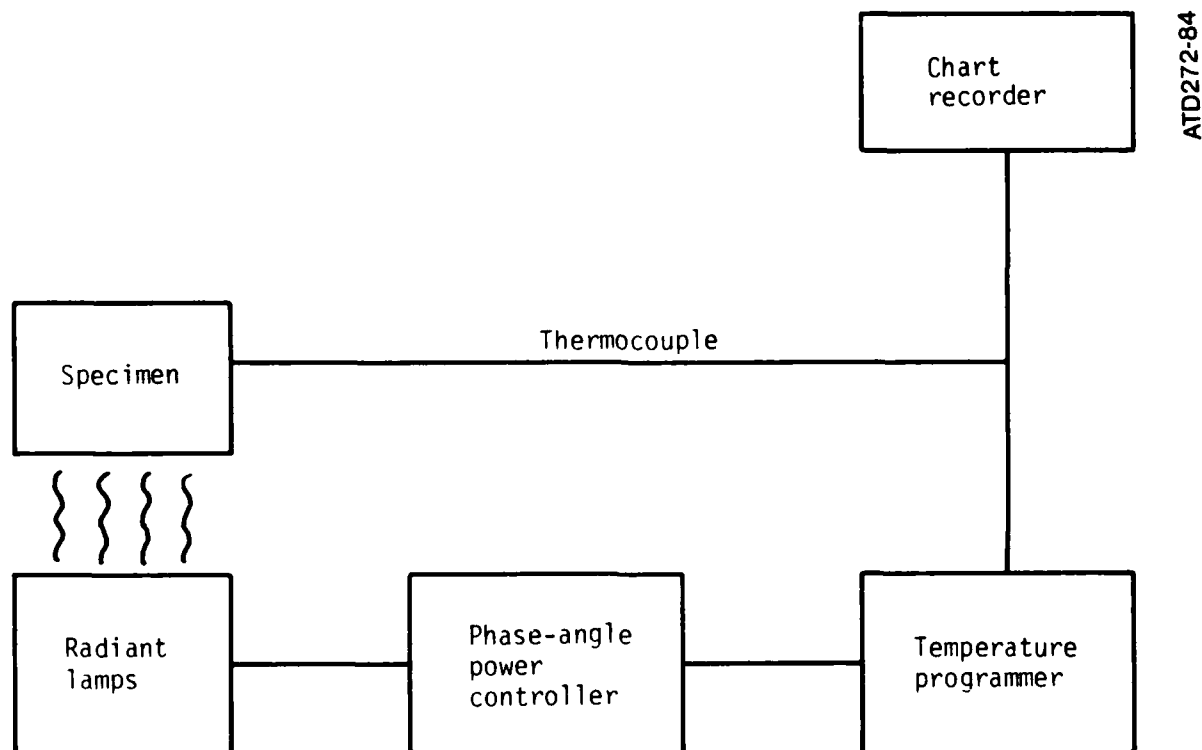


Figure 15. Wiring diagram

was conducted in a nitrogen atmosphere to prevent oxidation. When used, the test tube was rotated about its axis (vertical) at 10 to 15 rpm with the use of an electric motor and belt system. A circular, sliding-contact mechanism was used at the top of the tube for the thermocouple wires. For samples with graphite fiber bundles, Hercules HM 1000 PAN fibers were used.

After pyrolysis, each test tube was sectioned appropriately and prepared for microscopic observation. Depending on the type of sample and the use of rotation, the test tube was sectioned (Figure 16) either on a plane perpendicular to the magnetic field direction or on a plane perpendicular to the axis of the test tube (the rotation axis). The mesophase samples were vacuum impregnated with epoxy and polished. Optical micrographs were taken with a Zeiss Neophot 21 reflected-light microscope.

The test matrix for the pyrolysis runs for samples of petroleum pitch and/or graphite fiber bundles is given in Table 1. Initial runs were designed to determine the effect of the magnetic field on the mesophase transformation -- the alignment of spherules to the alignment of bulk mesophase. The effect of the alignment of the pitch matrix in a graphite fiber bundle was then investigated. Rotation was used to provide the highest degree of alignment. These initial pyrolysis runs indicated that indeed the magnetic field did align the mesophase. However, the magnetic field strength did not appear high enough and bubble percolation of escaping volatile gases tended to disrupt any alignment introduced by the magnetic field. Alinco permanent magnets of high magnetic strength were added to the large C-magnet to increase the magnetic field strength from 2000 to 5500G. Also, the pitch-fiber samples were slow cooled from the maximum pyrolysis temperature to allow alignment by the magnetic field without interference from bubble percolation.

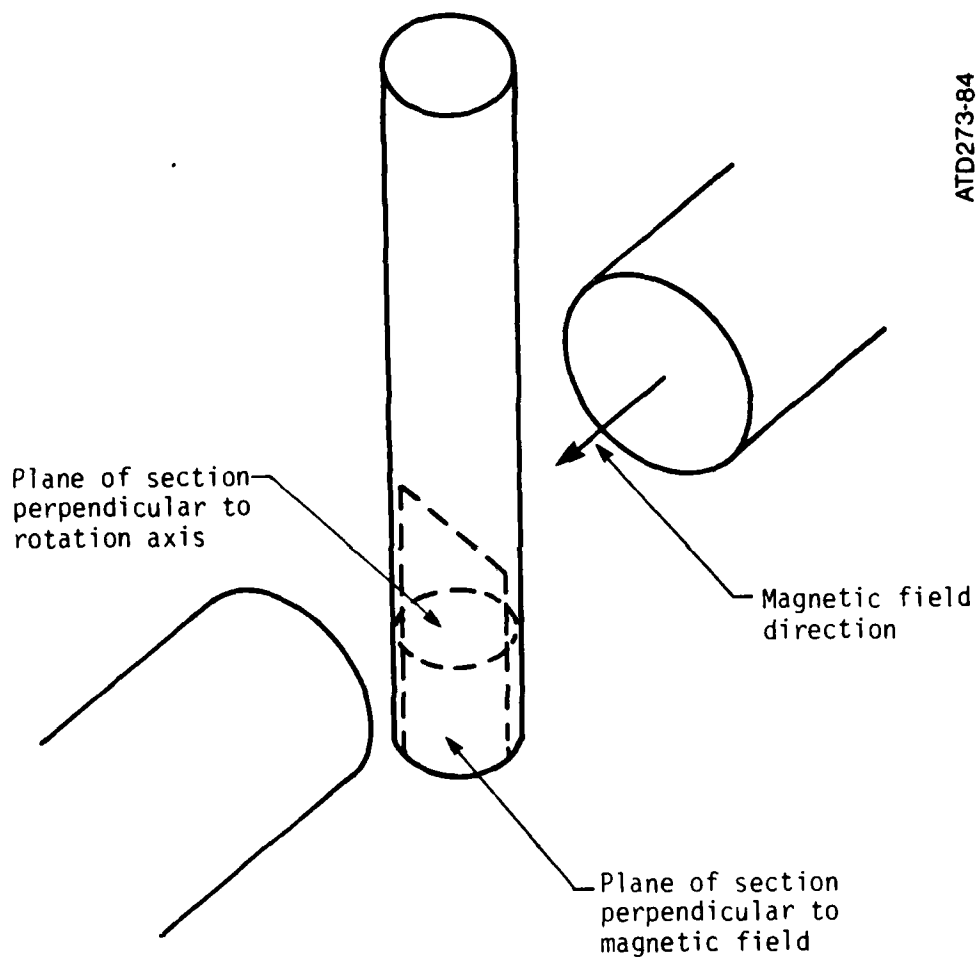


Figure 16. Sectioning plan

Table 1. Test Matrix

Run Number	Sample	Maximum Temperature ^a	Magnetic Field	Rationale
1	A240 pitch	420°C	2000G	Orientation of spherules
2	A240	440°C	✓	Effect on fresh mesophase
3	A240	460°C	✓	Effect on deformed mesophase
4	A240	480°C	✓	↓
5	A240	500°C	✓	Comparison to mesophase with magnetic field
6	A240	420°C		↓
7	A240	440°C		
8	A240	460°C		
9	A240	480°C		
10	A240	500°C		
11	HM pan bundle in A240 parallel to field	500°C	✓	Alignment in bundle
12	Bundle $\perp \bar{H}$	500°C	✓	Perpendicular alignment
13	// \bar{H}	500°C		For comparison
14	$\perp \bar{H}$	500°C		For comparison
15	$\perp \bar{H}$	500°C	✓	With rotation of sample about axis of bundle to force single alignment direction
16	A240	420°C	✓	With rotation at lower temperature and lower viscosity
20	A240 pitch with bundle	460°C, slow cool	5500G	Rotation about fiber axis, slow cool to prevent disruption by bubble percolation
22	A240 pitch	460°C, slow cool	✓	Alignment of mesophase
24	A240 pitch, pitch-fiber fabric	460°C, slow cool	✓	Alignment of matrix in bidirectional composite

RESULTS

The carbonaceous mesophase, a discotic nematic liquid crystal, is comprised of large aromatic molecules which are diamagnetic. This research has shown that the mesophase can be aligned by a magnetic field and that some degree of control can be introduced in developing the matrix microstructure in fiber bundles and composites. Presented here are the results highlighting the alignment by a magnetic field of the mesophase spherules, the bulk mesophase, the matrix with a graphite-fiber bundle and the matrix in a bidirectional fiber composite.

Alignment of Mesophase Spherules

The spherules are the first mesophase to form from the pyrolyzing petroleum pitch. These spherules are characterized by a layered structure in which the molecular layers all lie perpendicular to the polar axis of the spherule. Thus, in the magnetic field, the polar axes should all be in the plane perpendicular to the magnetic field direction (cf Figure 12). Mesophase spherules in the petroleum pitch pyrolyzed to 440°C are shown in the optical micrograph in Figure 17. These micrographs were taken with cross-polarized light to indicate the orientation of the molecular layer stacking of the mesophase. Rotation of the crossed polarizers aids in better definition of this structure. These micrographs show that the axes of the spherules lie in the plane of section which is perpendicular to the magnetic field direction.

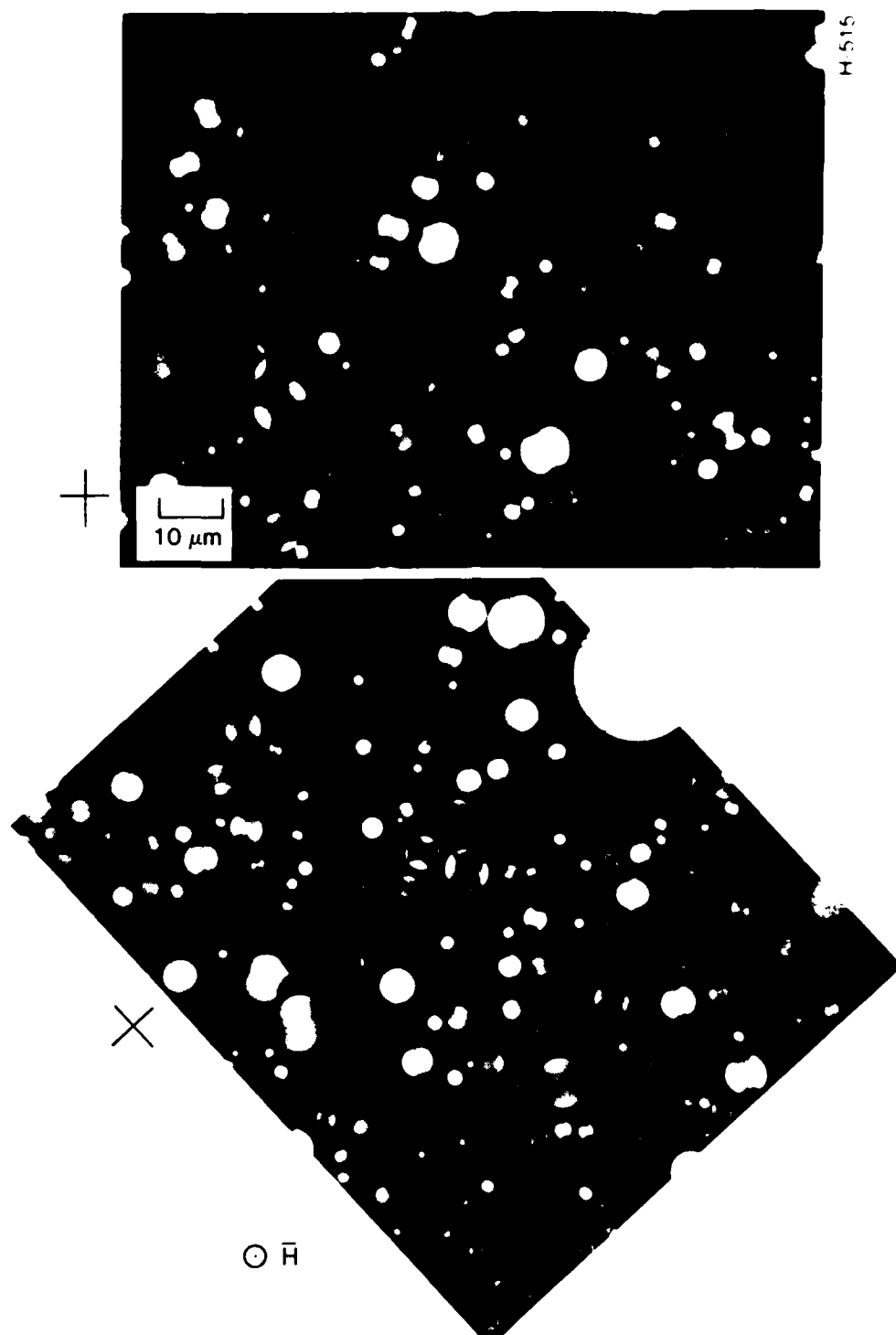
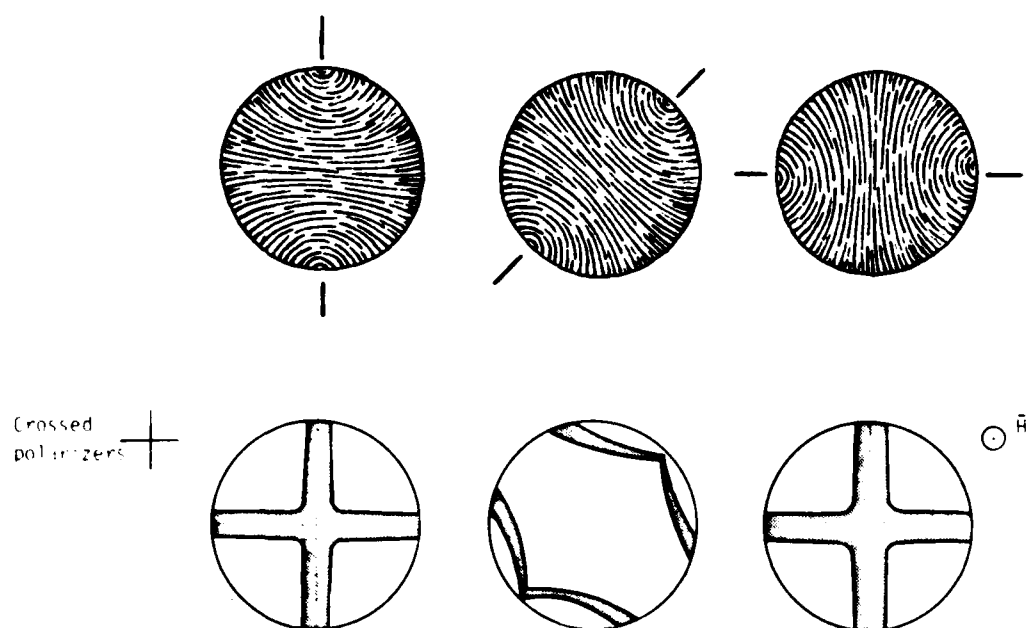


Figure 17. Optical micrographs of mesophase spherules aligned by magnetic field: 2000G, A240 pitch, 440°C

The extinction-contour patterns resulting from the cross-polarized light response of the mesophase spherules is shown schematically in Figure 18. The contours appear as a cross if the axis is perpendicular to a polarizing direction. They appear as curved chords of the circle if the axis is at an angle to the polarizers and the intersections of the chords denotes the poles. These extinction-contour patterns are present for the majority of the spherules in Figures 19 and 20, indicating that the spherules are aligned by the magnetic field.

Under similar pyrolysis conditions, but without the magnetic field, the mesophase spherules are randomly oriented. The extinction contours show the cross off center and there are spherules without the definite contours (Figures 21 and 22). When the polar axis is perpendicular to the plane of section, there is almost complete extinction of the spherule. This sample was sectioned on a plane oriented the same direction as the plane of section for the samples pyrolyzed in the magnetic field.

Rotation of the pitch sample in the test tube about its axis perpendicular to the magnetic field should align all the mesophase layers perpendicular to the rotation axis. Thus, the polar axes of the spherules should all be parallel to the rotation axis (cf Figure 12). Micrographs of these spherules pyrolyzed to 440°C are shown in Figure 23. Two planes of section are shown: perpendicular to the magnetic field direction and perpendicular to the axis of rotation. In the top micrograph, the poles axes are exactly parallel to the rotation axis. There is also some evidence of distortion of the spherules at the poles. At the poles, the molecular layers bend to lie perpendicular to the spherule surface and form a cuplike structure. The alignment by the magnetic field tends to flatten this cuplike structure and cause the sphere to distort to a more cylindrical shape. In the



ATD265-84

Figure 19. Extinction-contour patterns for Brooks-and-Taylor spherules oriented in a magnetic field

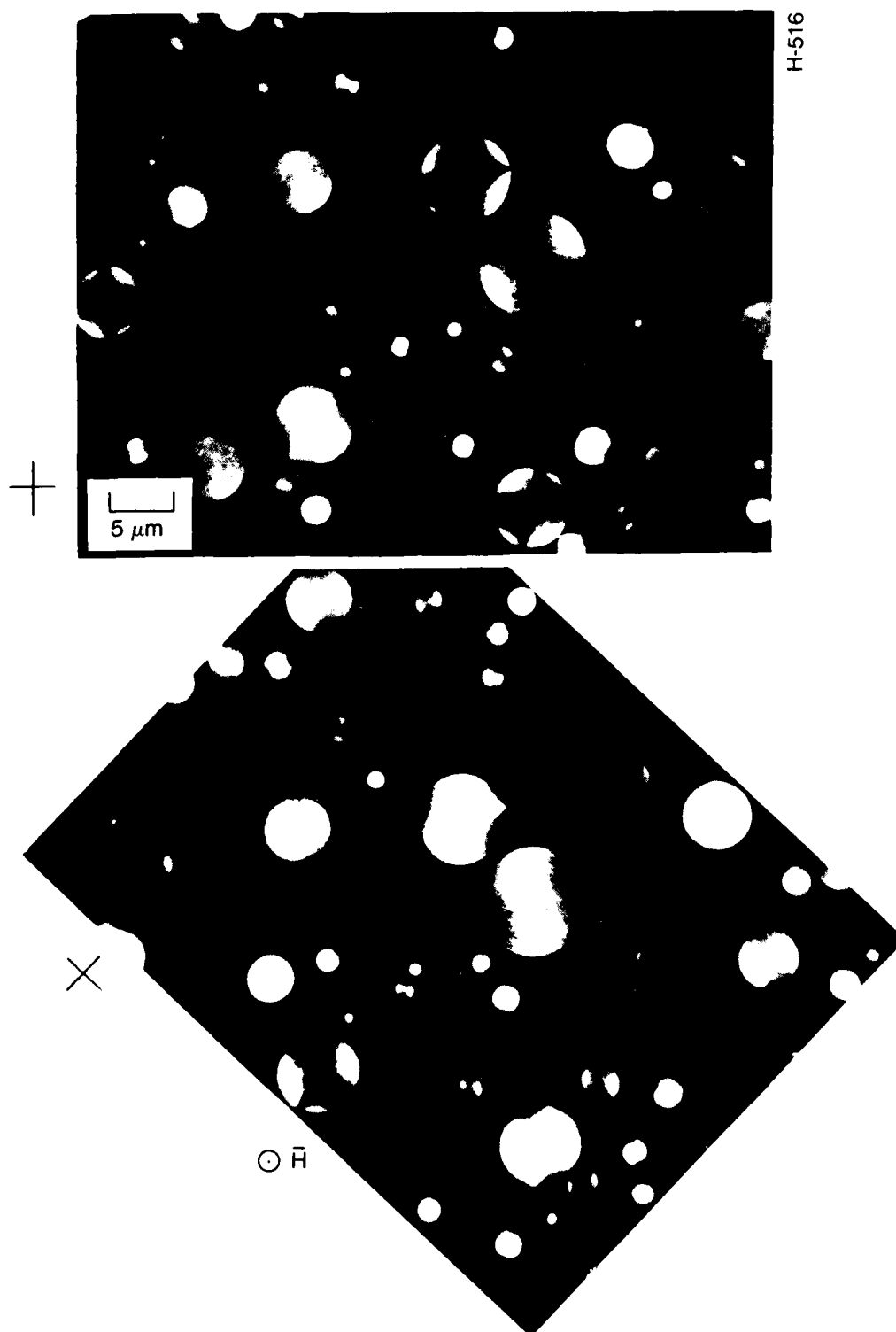
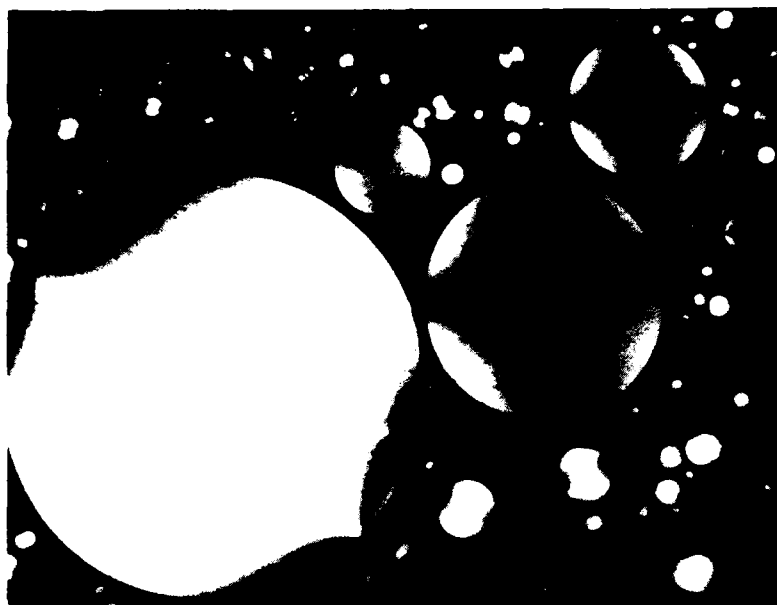
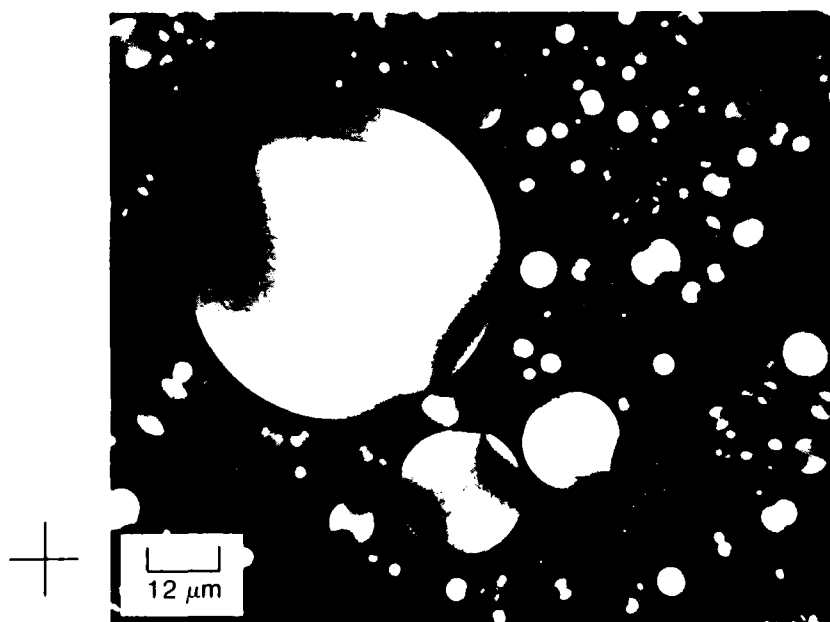


Figure 19. Optical micrographs of mesophase spherules aligned by magnetic field: 2000G, A240 pitch, 440°C



H-517



○ \vec{H}

Figure 20. Micrograph of spherules aligned in magnetic field

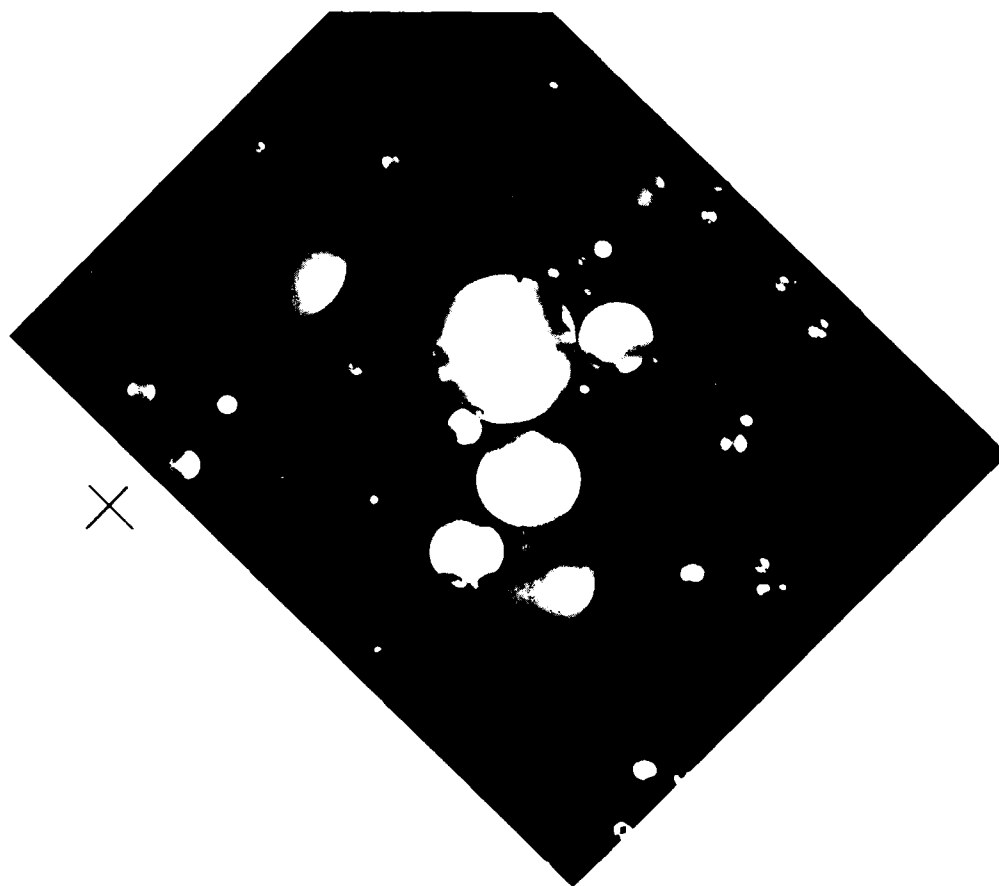
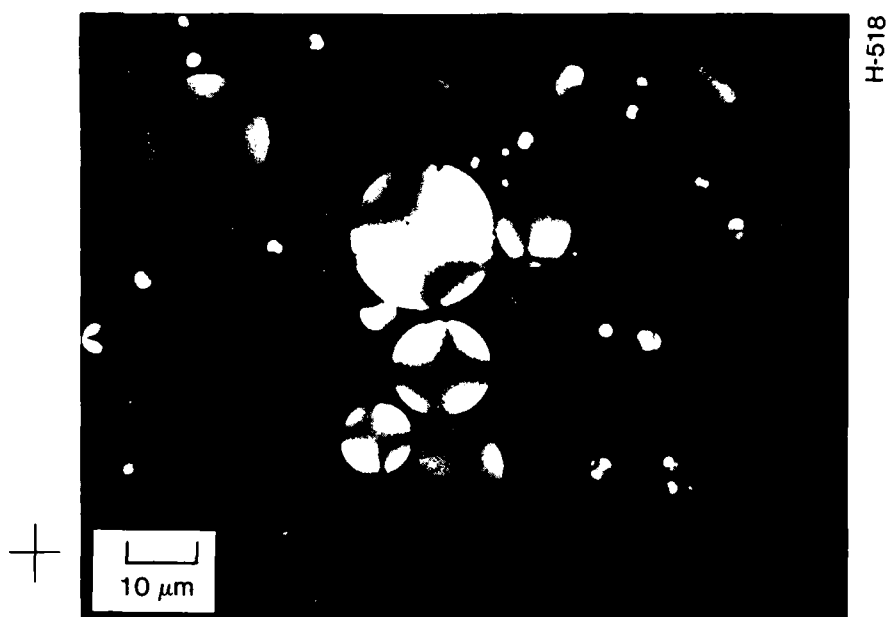


Figure 21. Micrographs of mesophase spherules formed in the absence of the magnetic field: A240 pitch, 440°C

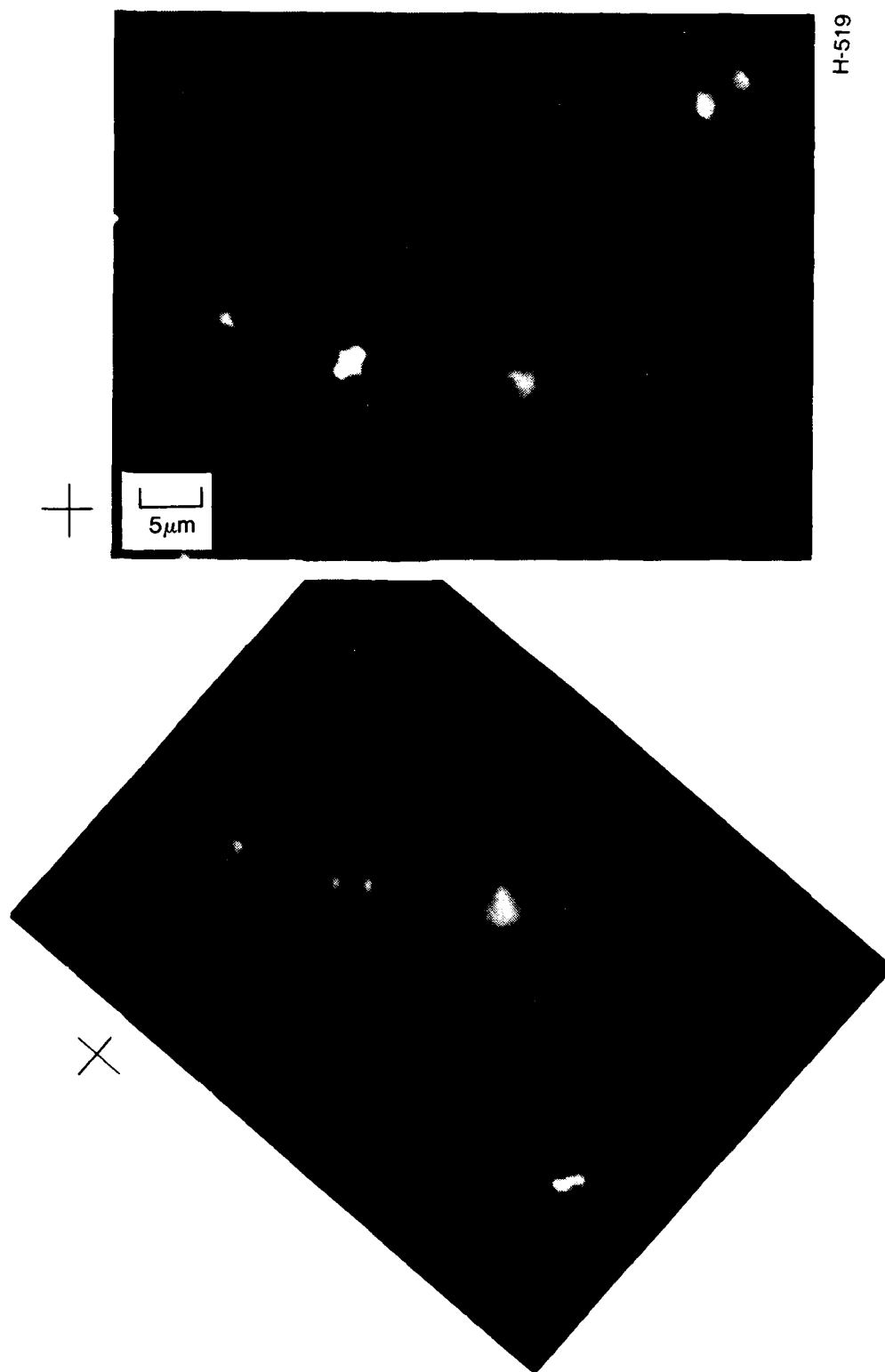
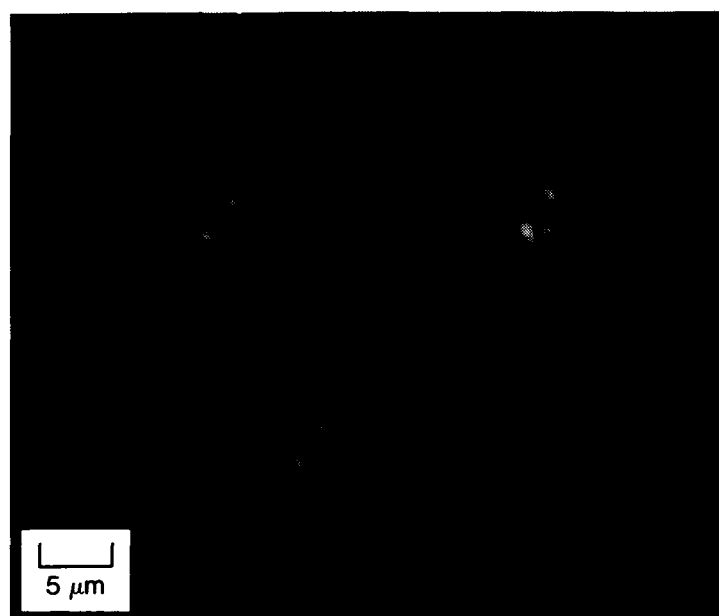


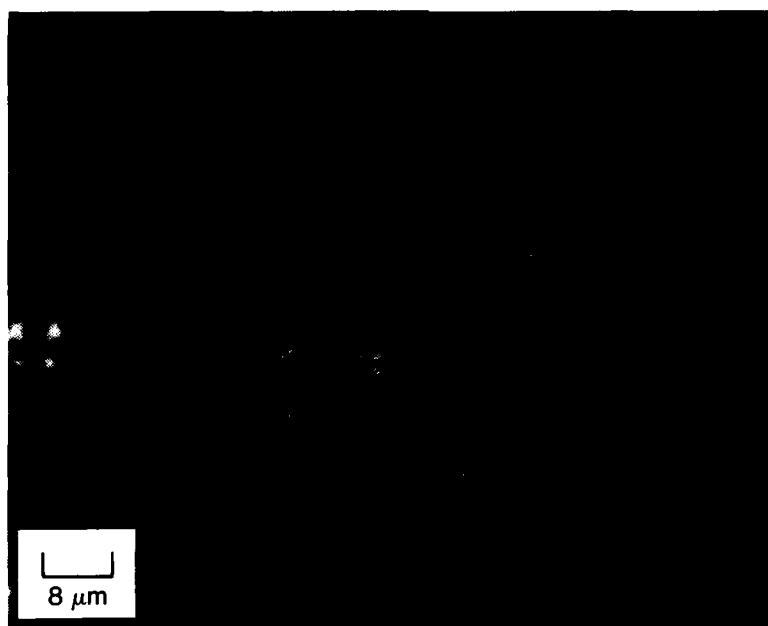
Figure 22. Spherules formed in the absence of the magnetic field



H=520

↑ rotation axis

⊙ H = 2000 gauss



↑ H = 5500 gauss

⊙ rotation axis

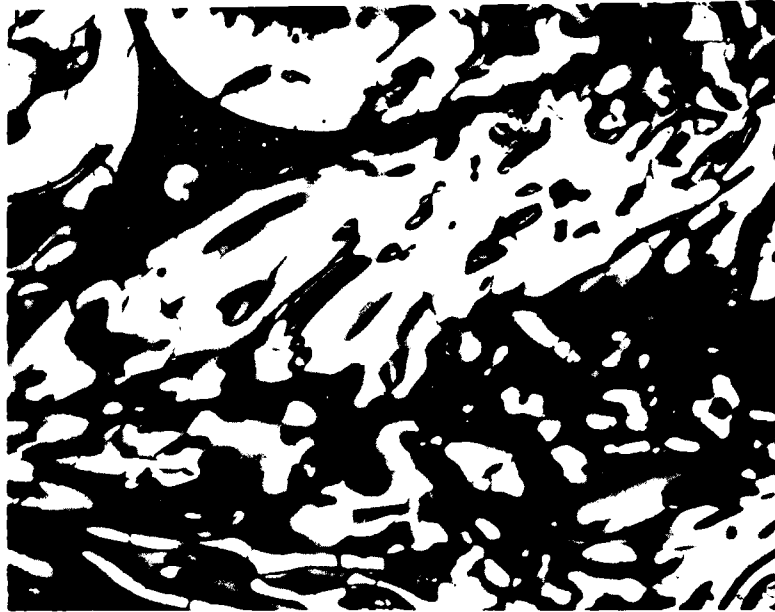
Figure 23. Single orientation of mesophase spherules from rotation of sample in magnetic field: A240 pitch, 420°C

bottom micrograph, the spherule axes are exactly normal to the plane of section. The extinction contour crosses result from a plane of section through the spherule between the pole and the equatorial plane. This plane of section reveals the circular structure of the cuplike layering. Although it is in complete extinction, there is one spherule in the upper left corner that has been sectioned on the flat equatorial plane.

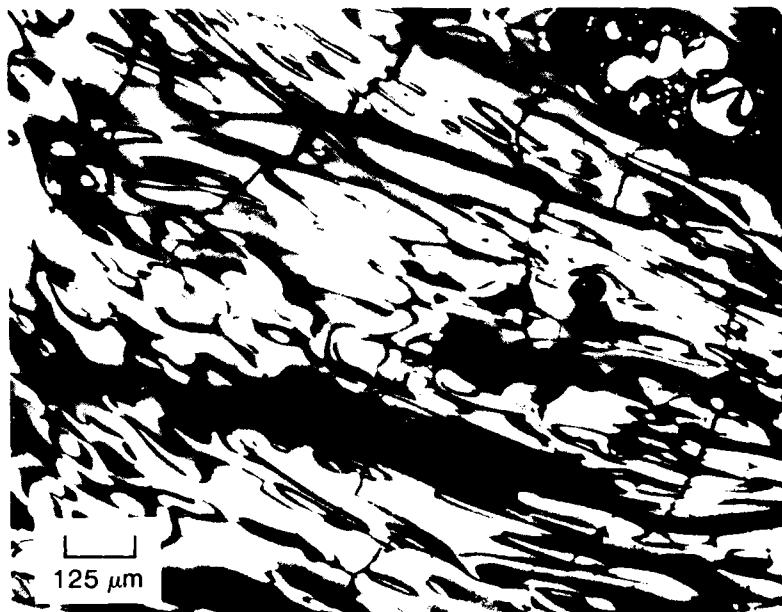
These micrographs show that the spherules of the carbonaceous mesophase are aligned by the magnetic field and that rotation of the sample can align the spherules in one specific orientation.

Alignment of Bulk Mesophase

On further heating of the petroleum pitch during pyrolysis, the mesophase spherules coalesce and form bulk mesophase. This bulk mesophase is the matrix of a carbon-carbon composite fabricated from such aromatic pitches, and alignment of this matrix and its disclination structures may lead to improved composites. The initial pyrolysis runs were done with the A240 petroleum pitch in a magnetic field of strength of 2000G. The pitch samples were heated slowly to 440°C and were not rotated. The bulk mesophase structure on the plane of section perpendicular to the magnetic field is shown in Figure 24. The structure is slightly deformed and there appears to be no distinct preferred orientation. In the magnetic field, all of the molecular layers should be perpendicular to this plane of section and all the disclinations should also be perpendicular to this plane of section. Figure 25 shows the plane of section parallel to the magnetic field. Here the mesophase layers are not parallel to the magnetic field as expected. Another pitch sample was pyrolyzed in the magnetic field and rotated about the vertical axis. Micrographs of the plane of section perpendicular to the rotation axis and shown in Figure 26. For this case, all the layers should be



H-521



$\odot \bar{H}$

Figure 24. Optical micrograph of bulk mesophase: 2000G, A240 pitch, 440°C



H-522

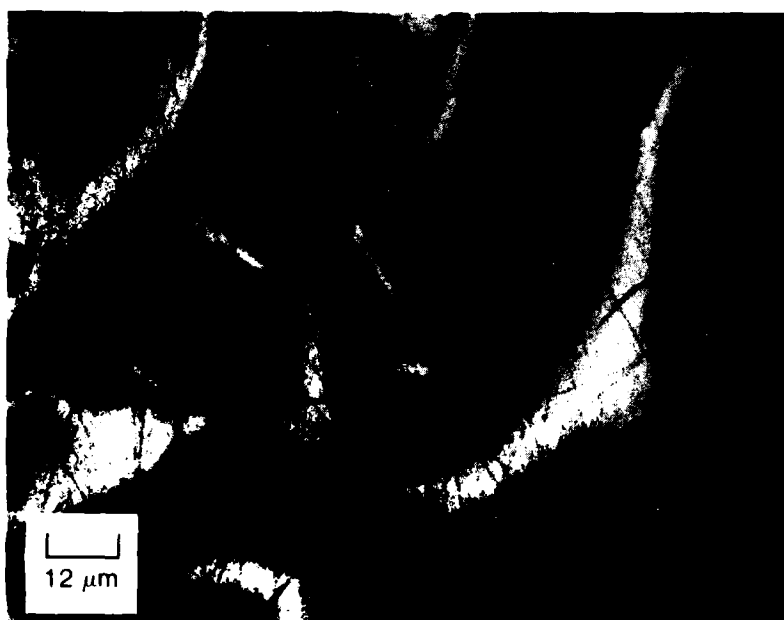


\vec{H}

Figure 25. Micrograph of bulk mesophase in 2000G magnetic field



H-523



○ Axis of rotation $\perp \bar{H}$

Figure 26. Micrographs of bulk mesophase rotated in magnetic field:
2000G, A240 pitch, 500°C

parallel to the plane of section. Such an orientation is not present. The mesophase structure appears slightly deformed and somewhat randomly oriented.

Two reasons are possible for this apparent lack of orientation of the bulk mesophase by the magnetic field. First, the strength of the magnetic field may not be high enough to orient a given mass of material. Thus, the permanent magnet was upgraded from 2000 to 5500G. Second, the deformed microstructures suggest that bubble percolation disrupted the mesophase structure that may have been introduced by the magnetic field. At the pyrolysis temperatures of interest, 420° to 500°C, there is a significant volatilization of lower molecular weight molecules and gas evolution from thermal cracking. These volatiles, as bubbles in the viscous mesophase, percolate through the mesophase to the surface. This passage of bubbles locally deforms the mesophase and the deformation energy apparently exceeds that of the energy of the alignment of the magnetic field. To alleviate this problem, all subsequent mesophase samples were cooled slowly after the maximum pyrolysis temperature was reached while still in the magnetic field. The reduction in temperature reduced volatilization and thermal cracking. Thus, the mesophase could be aligned by the magnetic field without interference by bubble percolation and before the mesophase has solidified.

The use of the magnetic field of strength of 5500G and the slow cooling resulted in alignment of the bulk mesophase by the magnetic field. The evidence of this alignment is shown in Figures 27 through 32. On the plane of section perpendicular to the magnetic field direction, the mesophase structure is characterized by the edges of layers normal to the plane of section. The disclinations present; at the nodes and crosses in the extinction contours, are oriented with the disclination line or core parallel to the magnetic field (Figures 27 and 28). Generally, the structures on this plane of section

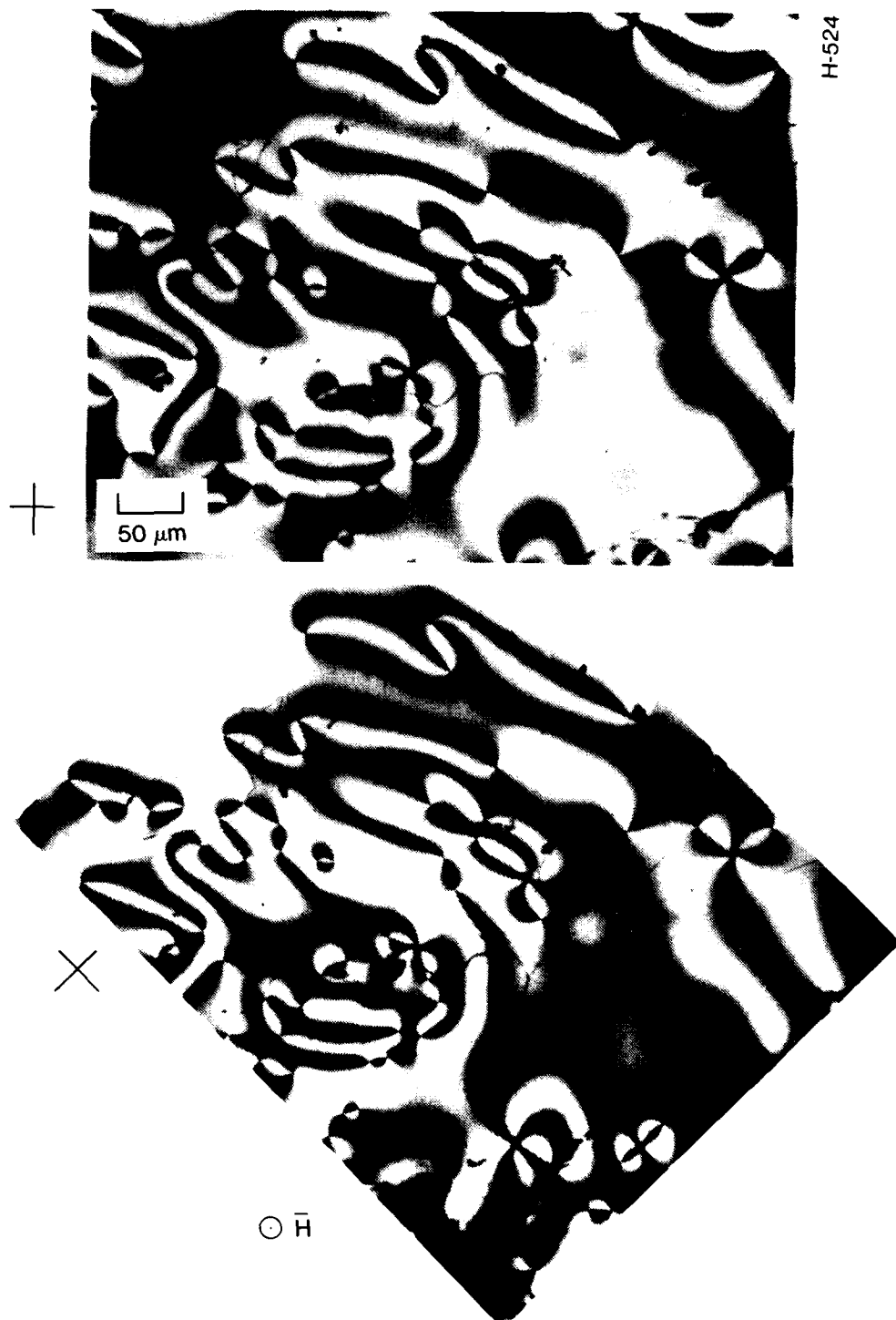


Figure 27. Optical micrographs of bulk mesophase aligned by magnetic field: 5500G, A240 pitch, 460°C, section perpendicular to field

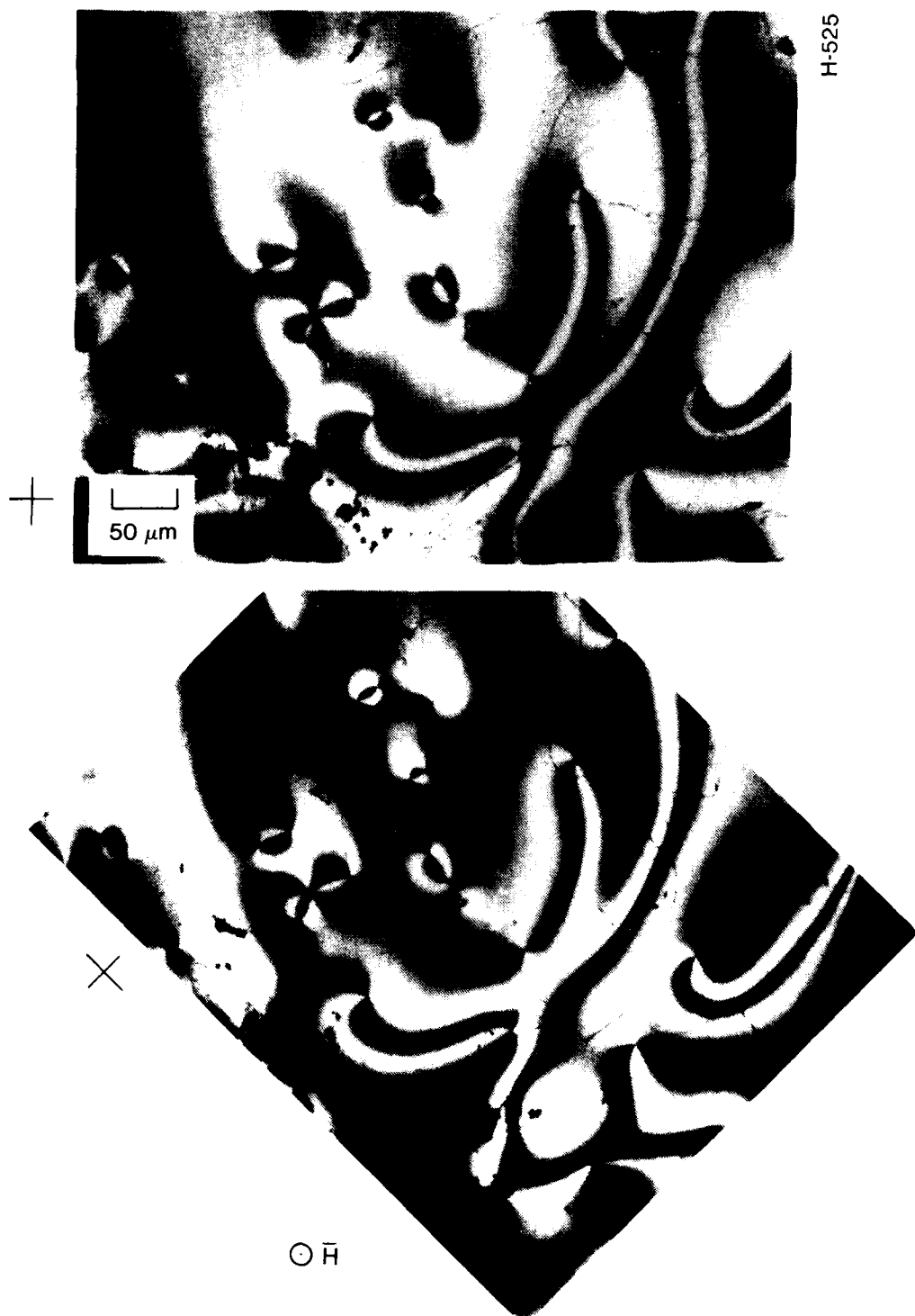


Figure 28. Micrographs of aligned bulk mesophase

appear isotropic; however, as shown in Figure 29, the remnant of deformation by perhaps bubble percolation is evident in aligning the mesophase layers to some degree. The layers are still perpendicular to the plane of section.

More revealing of this aligned microstructure are the micrographs on the plane of section parallel to the magnetic field (Figures 30 to 32). In Figure 30, the top micrograph shows almost complete extinction in the cross-polarized light. All the layer edges must be oriented horizontally. The micrograph at a 45° rotation of the polarizers shows these layers not in extinction. The remaining dark bands are folds in the molecular layers and the crease of the fold lies parallel to the magnetic field and in the plane of section. Figures 31 and 32 show this same high degree of alignment with some small imperfections such as the curved folds.

This microstructure of the bulk mesophase aligned by the magnetic field as determined by these micrographs on the two principal planes of section is schematically illustrated in Figure 33. This structure is the fibrous structure⁵ characteristic of uniaxial deformation of the mesophase and present in needle coke. All the layers are oriented such that the normal to the disklike molecules lie in the plane perpendicular to the magnetic field. This is the orientation shown in Figure 11. The disclinations present are wedge disclinations and they are all aligned parallel to the magnetic field. Thus, the matrix and its disclinations in a carbon-carbon composite could be aligned in this fibrous structure with the use of a magnetic field.

Alignment of Mesophase in Fiber Bundle

Without a magnetic field, the matrix microstructure with a graphite-fiber bundle in a carbon-carbon composite is controlled by the alignment of the disklike molecules parallel to the surface of the filaments. The wedge disclinations among the filaments result from the geometrical

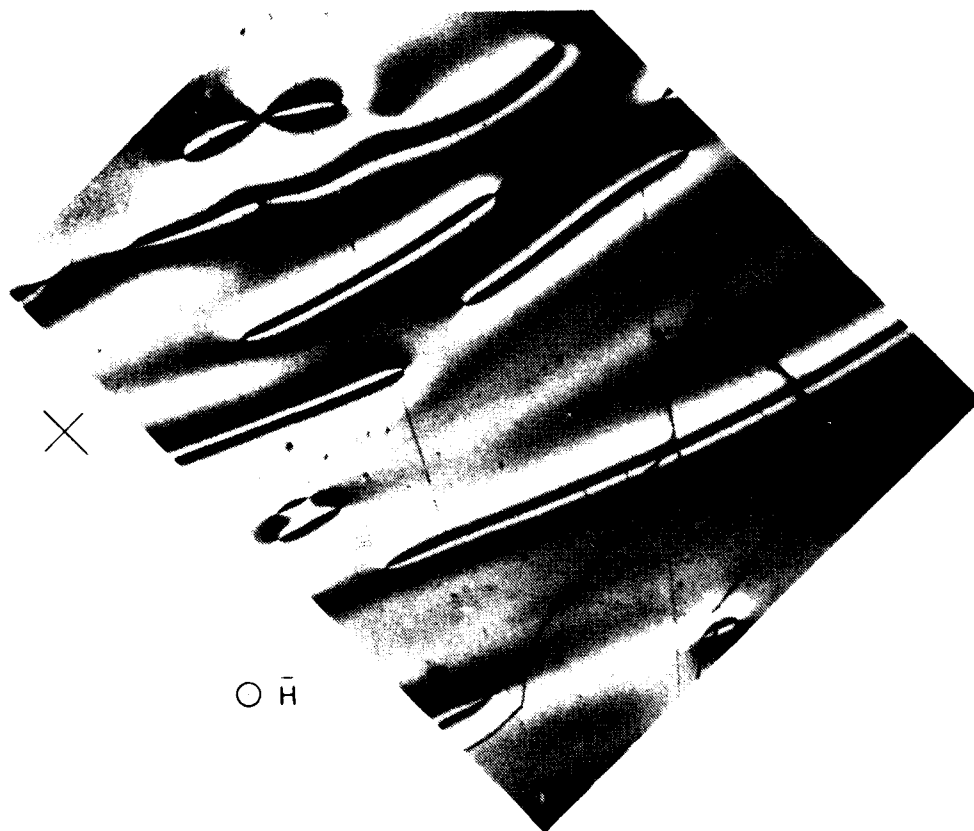


Figure 29. Micrographs of aligned bulk mesophase

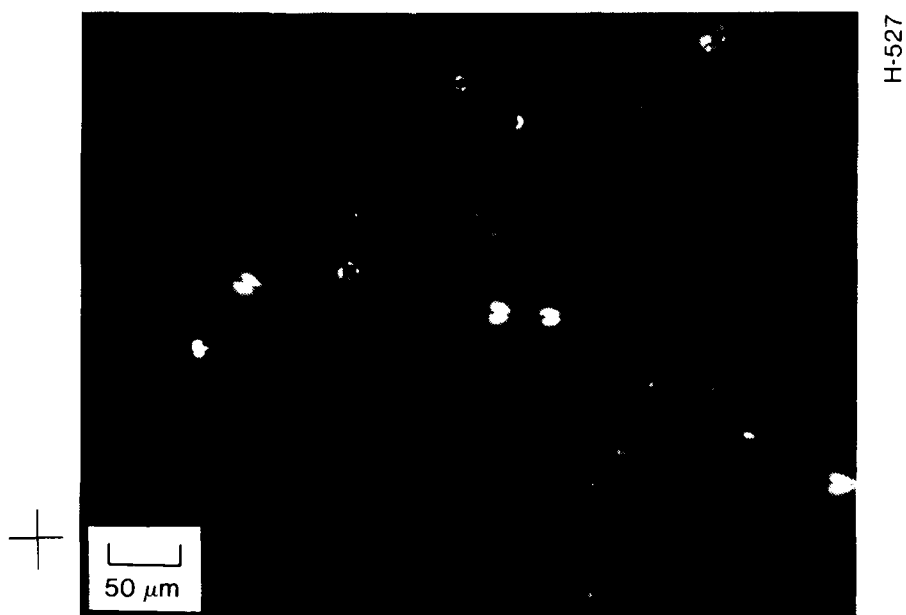


Figure 30. Micrographs of bulk mesophase aligned by magnetic field:
5500G, A240 pitch, 460°C, section parallel to field

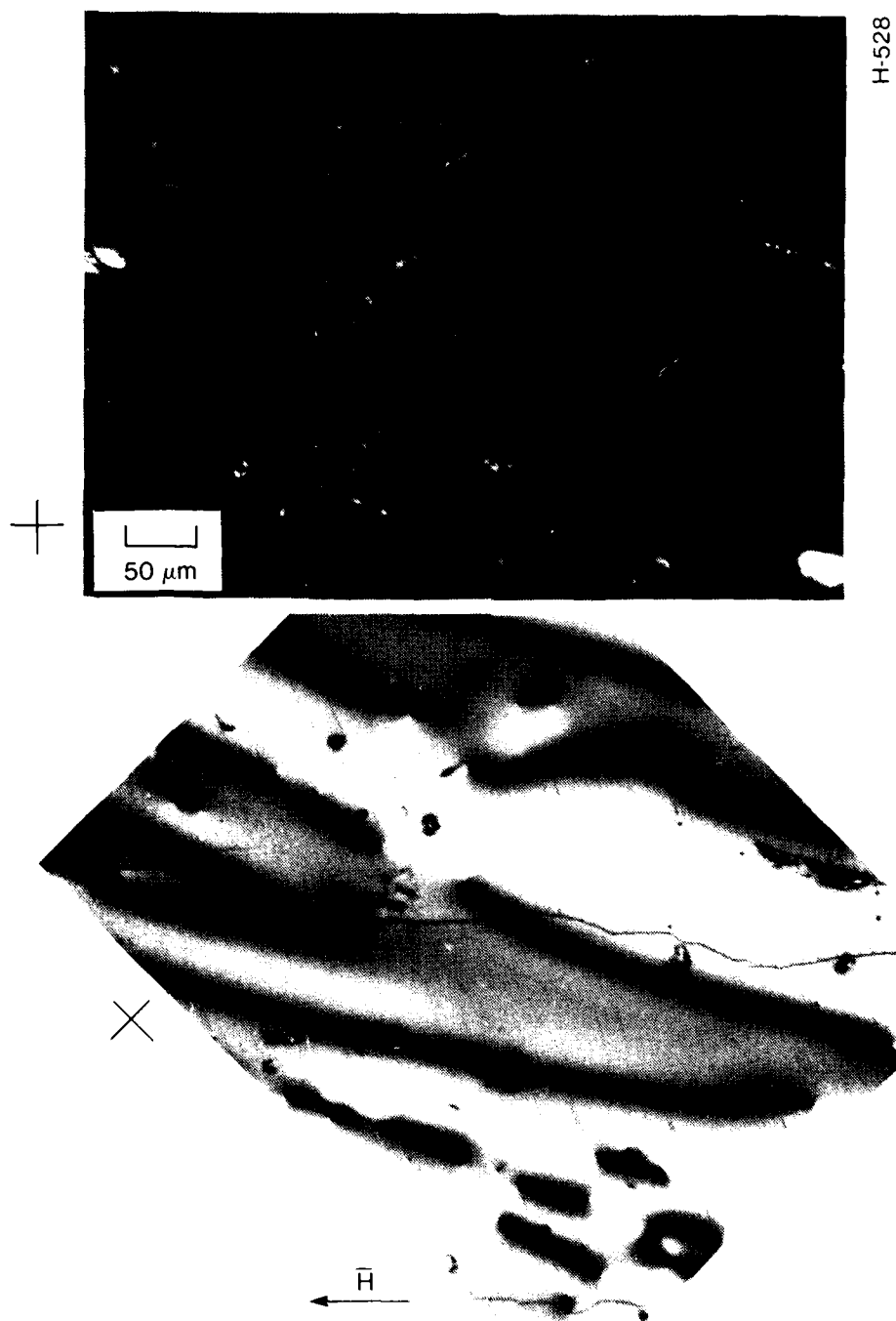


Figure 31. Micrographs of aligned bulk mesophase

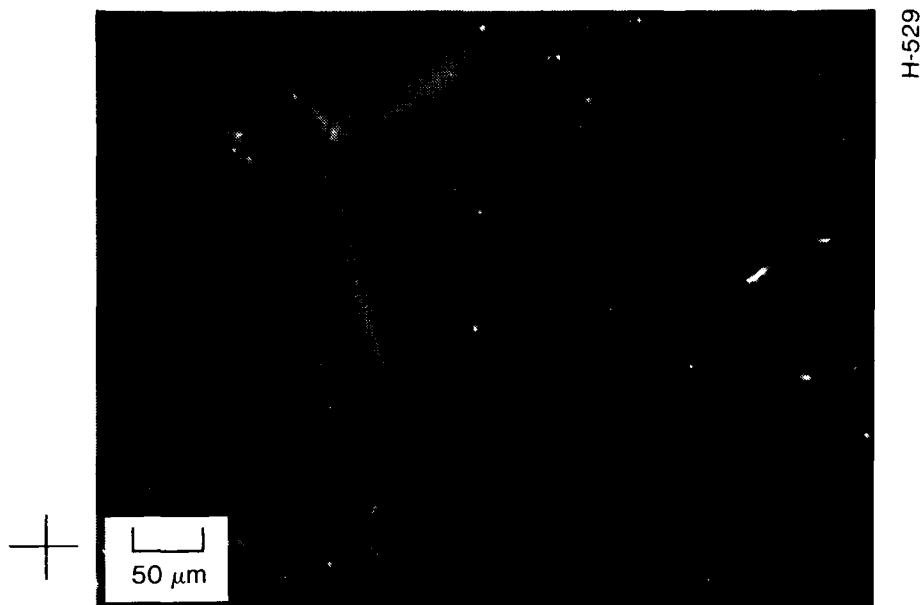


Figure 32. Micrographs of aligned bulk mesophase

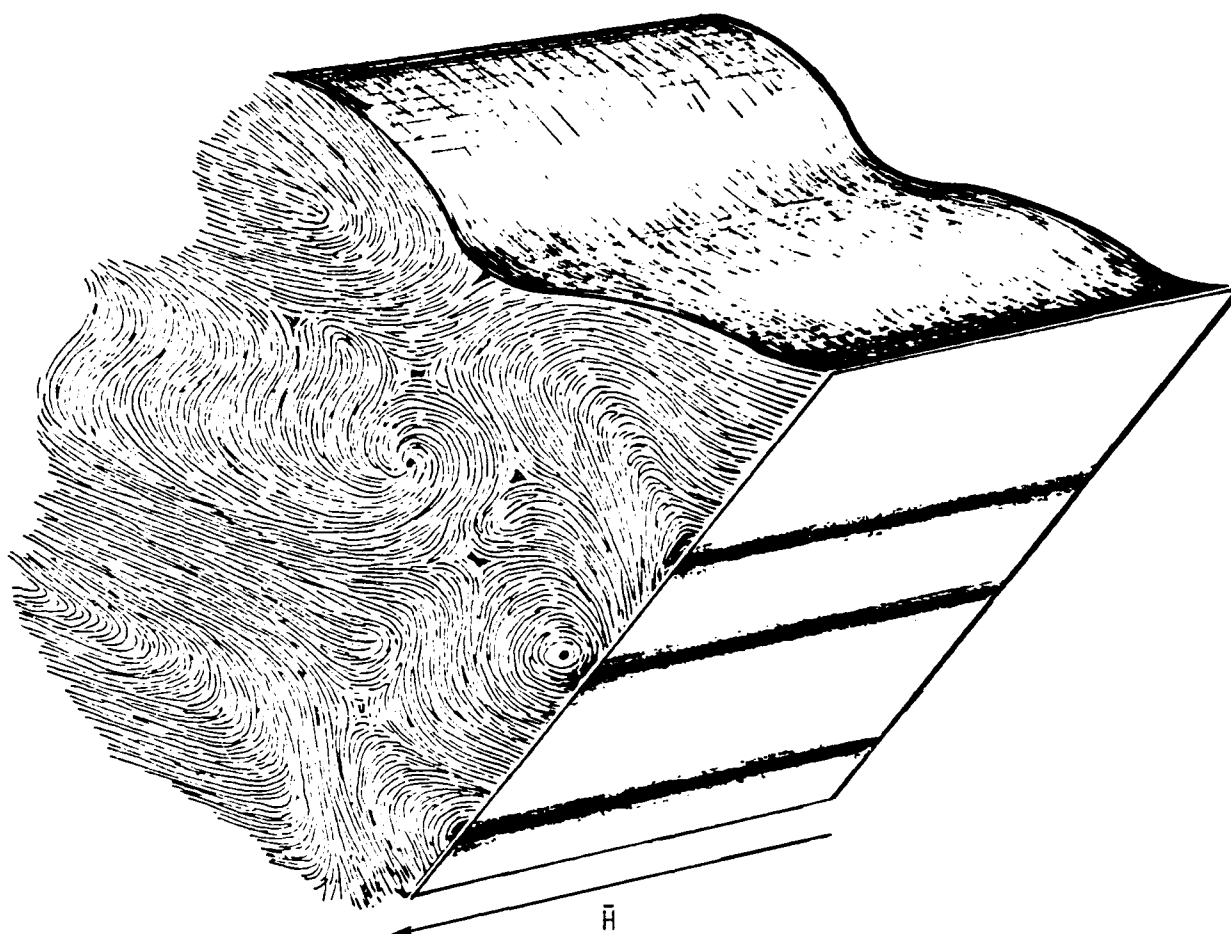
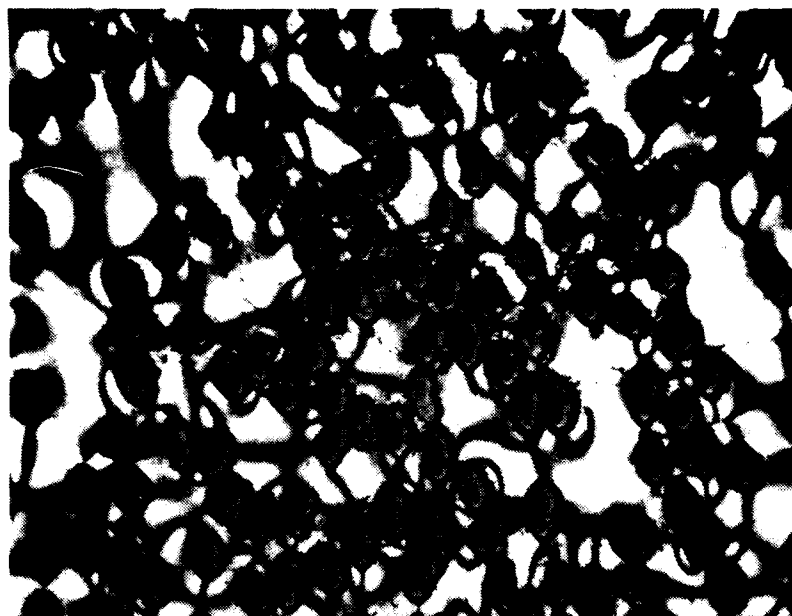


Figure 33. Schematic diagram of fibrous structure of bulk mesophase aligned by a magnetic field

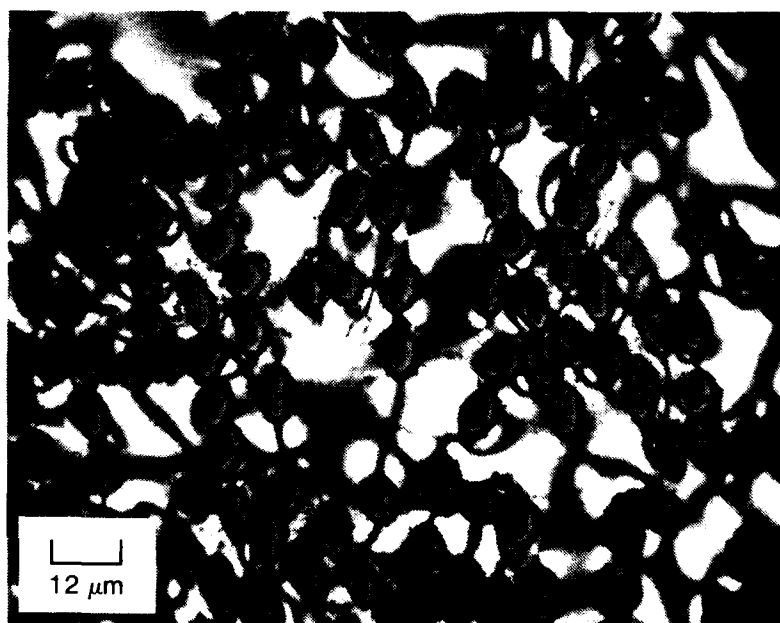
constraints of the various arrays of filaments and the oriented matrix about each filament.⁸ The use of the magnetic field during pyrolysis of the pitch in a fiber bundle may provide a means of altering this disclination structure. Three orientations of fiber bundle and magnetic field have been investigated: the magnetic field parallel to the bundle axis, the field perpendicular to the bundle axis, and rotation of the bundle about its axis in the magnetic field perpendicular to this rotation axis. The filaments used were Hercules HM PAN and Union Carbide T300 PAN filaments. These are 7 μm diameter filaments with circular (HM) and kidney-shaped (T300) cross sections.

Optical micrographs of the fiber bundle pyrolyzed with the magnetic field parallel to the bundle axis are shown in Figure 34. For this case, the magnetic field aligns the molecules in the same direction as the fiber surfaces. Thus, there is no distinct change in the matrix microstructure within the bundle (cf Figures 5 and 6). In the saddle-shaped cores of the disclinations of strength $S=-1$, there are molecules oriented perpendicular to the filaments (Figure 7). The parallel magnetic field would tend to reorient these perpendicular molecules in the center of the core to lie parallel to the disclination line (parallel to the filament direction). The evidence of this would be an extinction-contour cross in which the contours are pinched down and meet at a well-defined point (no saddle-shape core), or the $S = -1$ disclination may separate to two $S = -1/2$ disclinations with parallel alignment throughout the core. The crosses, however, still display rather broad, diffuse centers representative of the saddle-shaped cores.

For the fiber bundle oriented perpendicular to the magnetic field (Figure 35), there again appears to be little effect of disrupting the sheathlike alignment of the molecules parallel to the filament surfaces. Disclinations are present and they do not appear distorted in any way. This

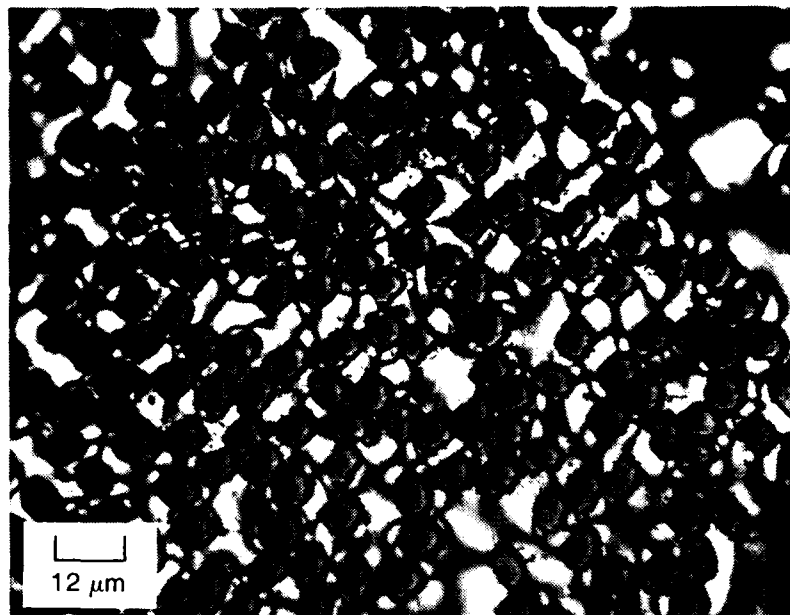


H-530

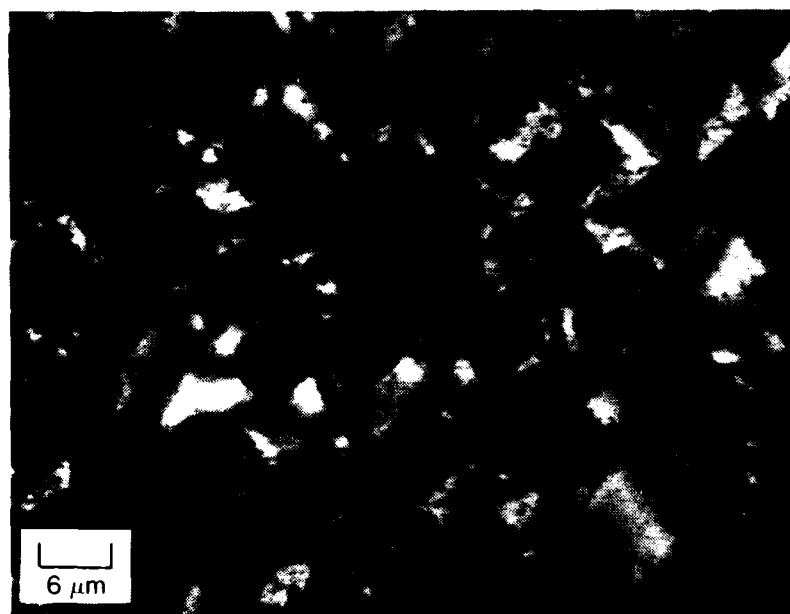


$\odot \bar{H}$

Figure 34. Micrographs of T300 fiber bundle parallel to magnetic field:
5500G, A240 pitch, .460°C



H-531



\vec{H} →

Figure 35. Micrographs of fiber bundle perpendicular to magnetic field

figure shows a region of tightly packed filaments. In regions where the packing is open and larger regions of bulk mesophase exist, there is definite alignment of these matrix areas, as shown in Figure 36. The layers lie parallel to the magnetic field and parallel to the fiber direction.

The competition between the alignment of the disklike molecules by the filament surfaces and the alignment by the magnetic field is dramatically illustrated for the fiber bundle rotated in the magnetic field. For this case, all the mesophase molecules aligned by the magnetic field should lie perpendicular to the filament. This is the case, as shown in Figures 37 and 38, for the bulk mesophase surrounding the tightly packed filaments. But within the fiber bundle itself, the alignment by the fiber surface dominates. Figures 39 and 40 show that the dark areas do not change with rotation of the crossed polarizers, indicating that in these areas the molecular layers are parallel to the plane of section and perpendicular to the bundle axis and the axis of rotation. The layers around each filament are oriented parallel to the surface as a sheath. This is evident in the extinction-contour cross pattern in the white ring about the isolated filaments in Figures 39 and 40.

The alignment of the disklike molecules parallel to a surface stems from geometrical factors and possible chemical factors. Forces acting on the molecules by the surface produce this strong anchoring of the molecules. This anchoring energy is thus larger than the energy induced by the magnetic field. The relationship between the orientational torques due to the anchoring and the magnetic field can reveal information about the elastic behavior of this discotic liquid crystal. This is described next.

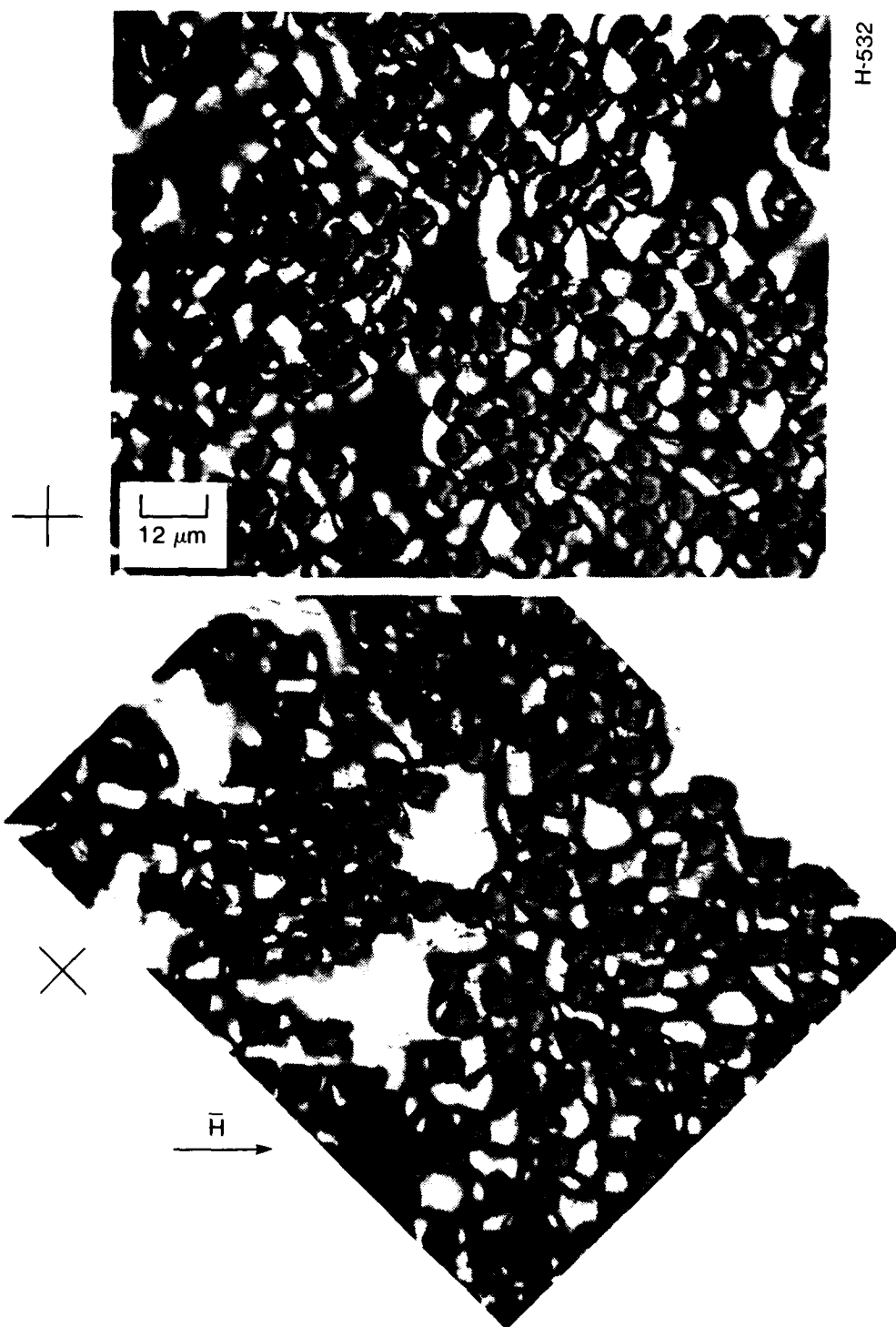
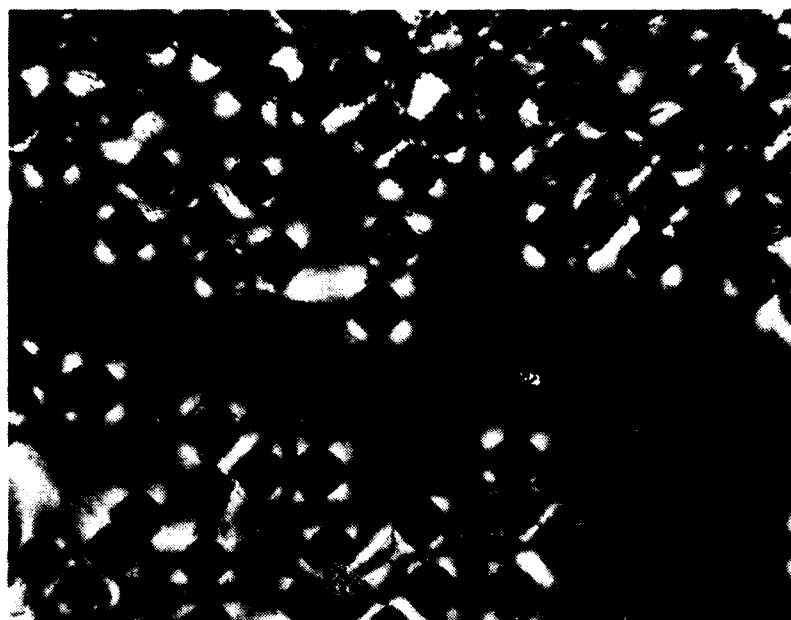
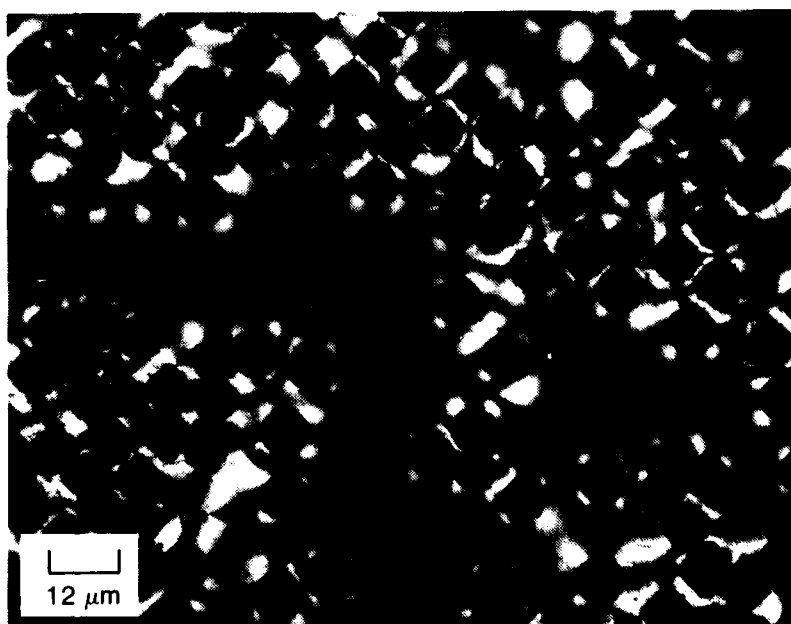


Figure 36. Micrographs of fiber bundle perpendicular to magnetic field



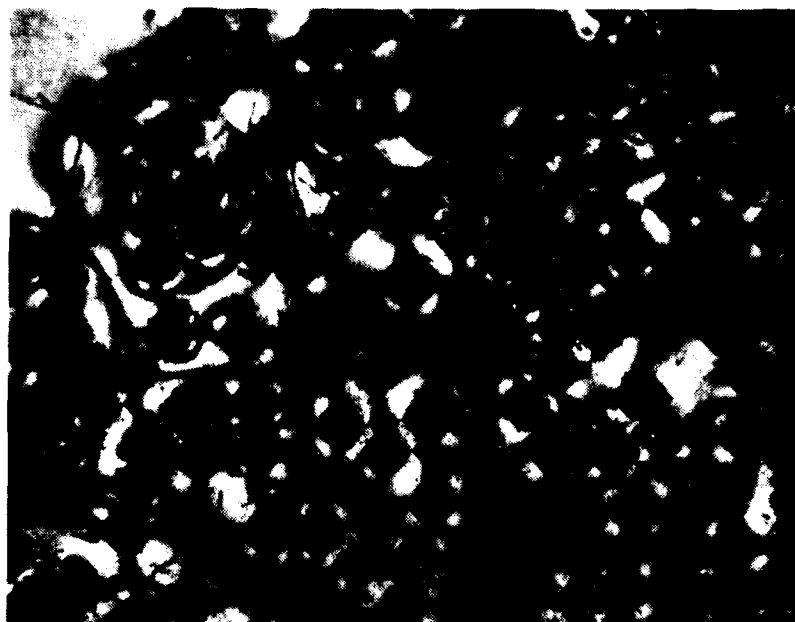
H-533



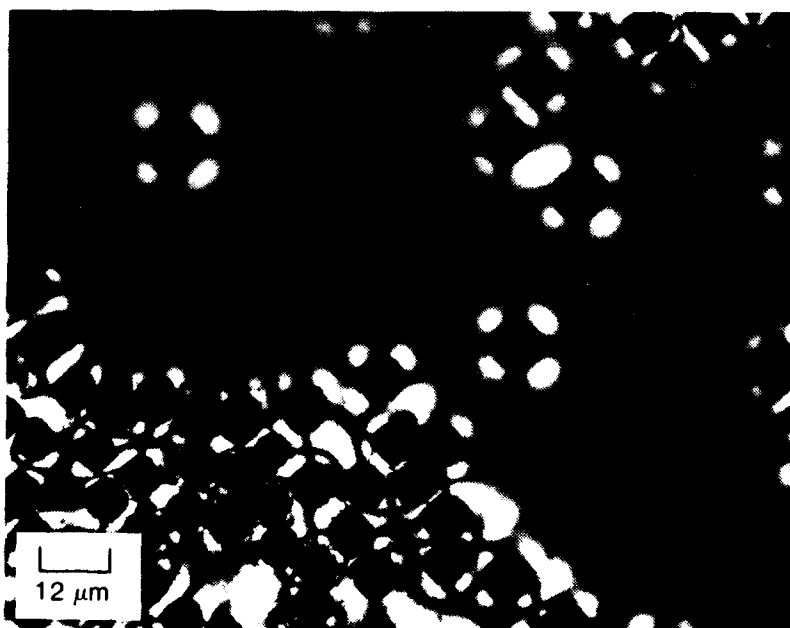
⊙ rotation axis

\vec{H} →

Figure 37. Micrographs of HM fiber bundle rotated in magnetic field perpendicular to the axis of rotation



H-534



⊙ rotation axis

\vec{H} →

Figure 38. Micrographs of fiber bundle rotated in magnetic field perpendicular to bundle axis

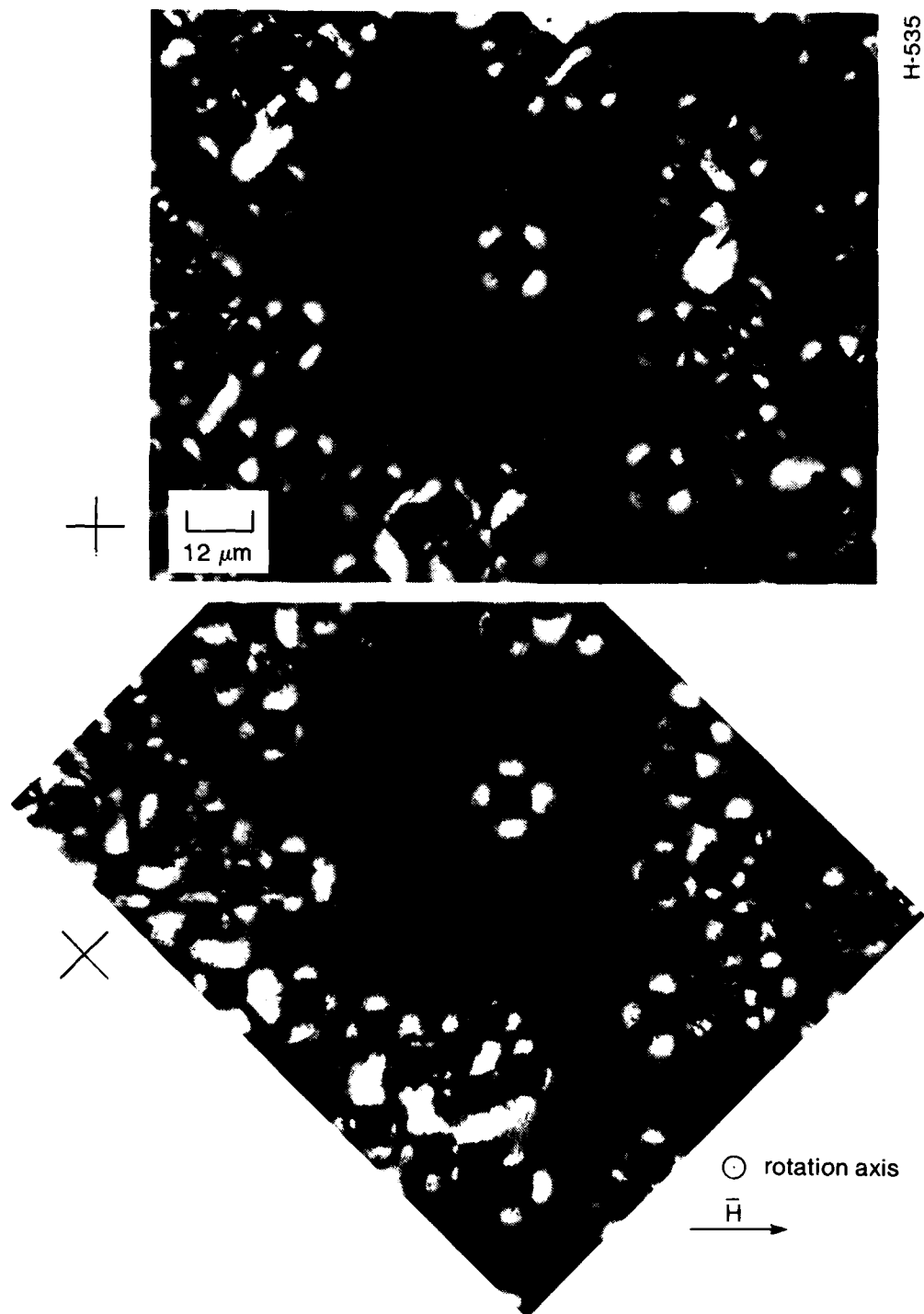


Figure 39. Micrographs of rotated fiber bundle showing alignment of bulk mesophase perpendicular to axis

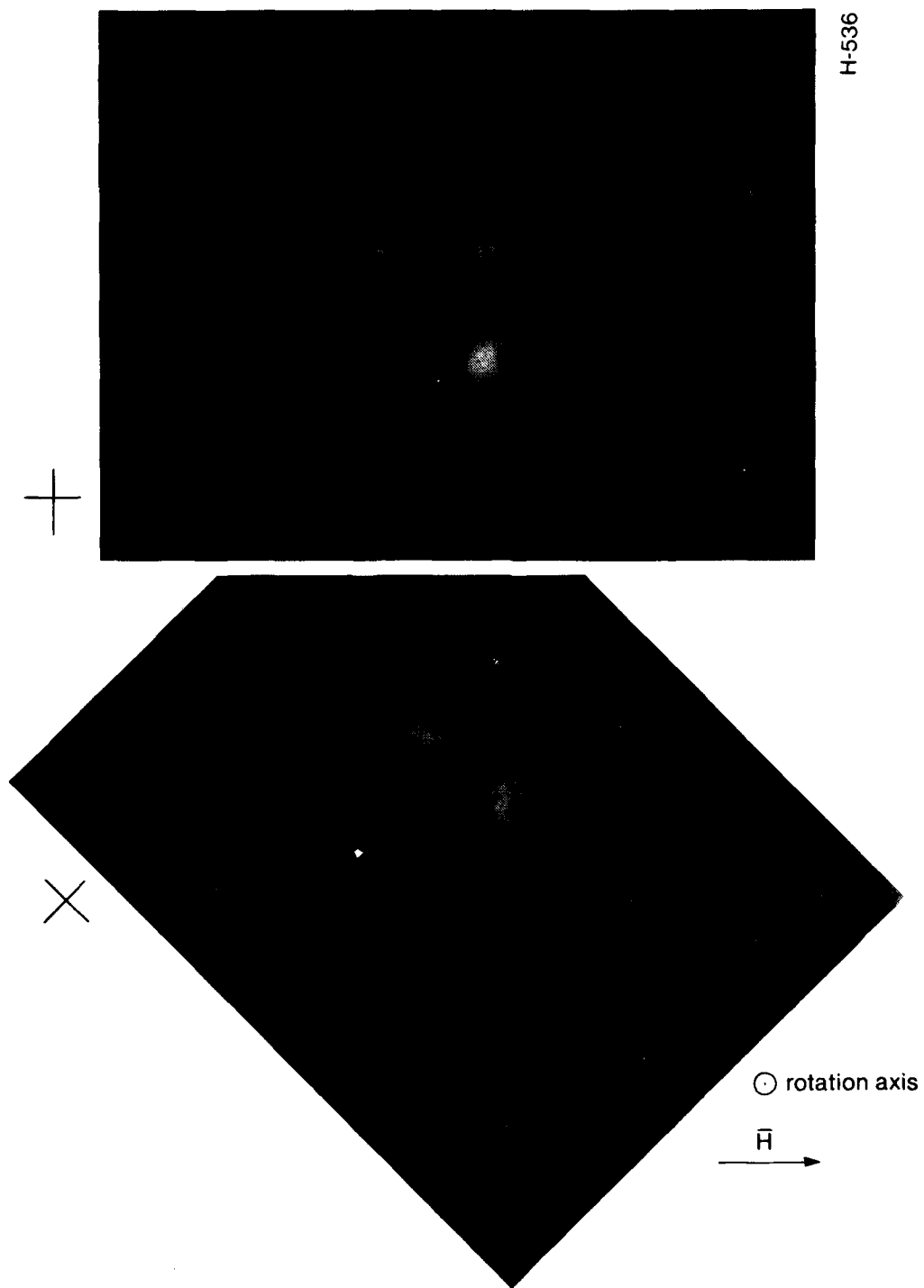


Figure 40. Circular sheath about individual filament with bulk mesophase perpendicular to filament

Magnetic Coherence Length and Bend Elastic Constant

For the competing effects of strong anchoring at the surface and the magnetic field, the molecular orientation changes as shown in Figure 41. This curvature is bend and is one of three curvatures possible for a liquid crystal. (The other two are splay and twist.¹³) The surface exerts a torque on the material away from the wall; this torque is related to the elastic constant K_3 for bend. This elastic constant is a measure of the resistance of the liquid crystal to bend as a result of some external force. The magnetic field also exerts a torque on the bulk liquid crystal. This torque is related to:

$$\tau \sim \chi_a H^2$$

where χ_a is the difference in the parallel and perpendicular diamagnetic susceptibilities and H is the magnetic field strength. A length can be defined over which these two torques balance. This length is called the magnetic coherence length:¹³

$$\xi = \left(\frac{K_3}{\chi_a} \right)^{1/2} / H$$

This magnetic coherence length is the thickness of the white ring about the filaments in Figures 37 through 40. Both the diamagnetic anisotropy of the carbonaceous mesophase and the magnetic field strength are known. Thus the elastic constant for bend for the carbonaceous mesophase can be determined. For

$$\xi = 7 \pm 1 \text{ } \mu\text{m}$$

$$\chi_a = -0.69 \times 10^{-6} \text{ emu/g}$$

$$H = 5500\text{G} = 5500 \text{ oersteds},$$

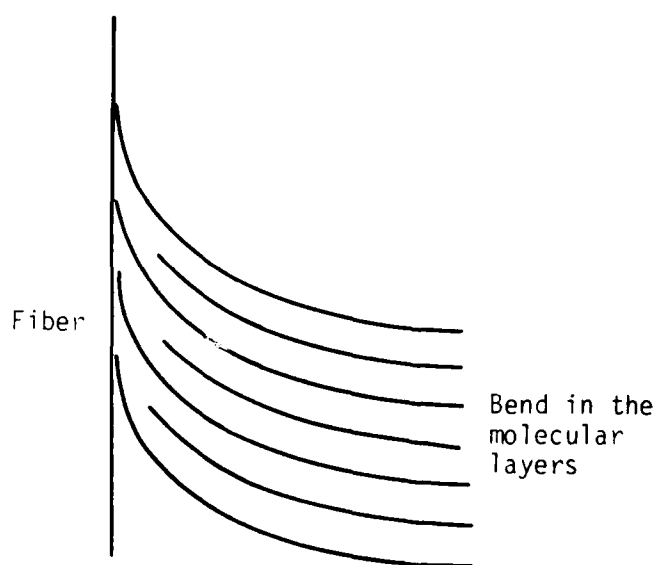
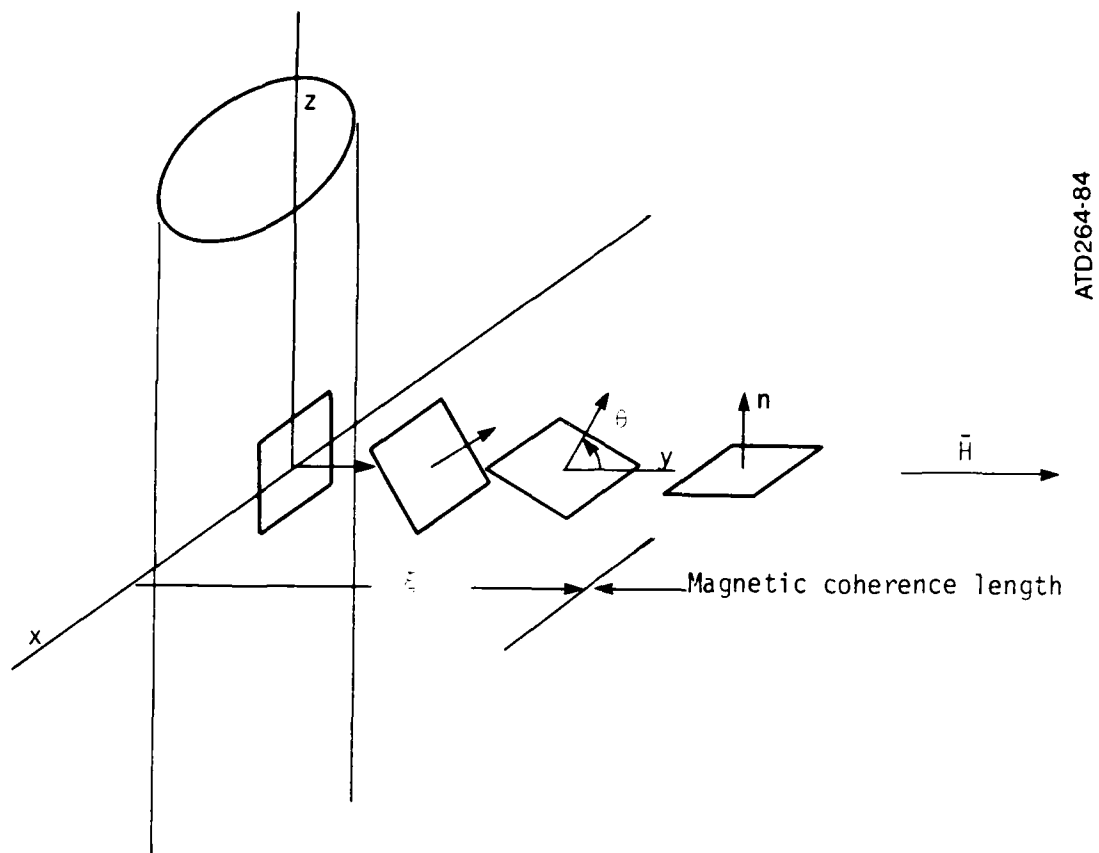


Figure 41. Orientation of molecules anchored at filament surface and oriented by magnetic field

then

$$K_3 = 10^{-5} \text{ dynes.}$$

The elastic constants for bend for the conventional rodlike nematic liquid crystals¹³ are

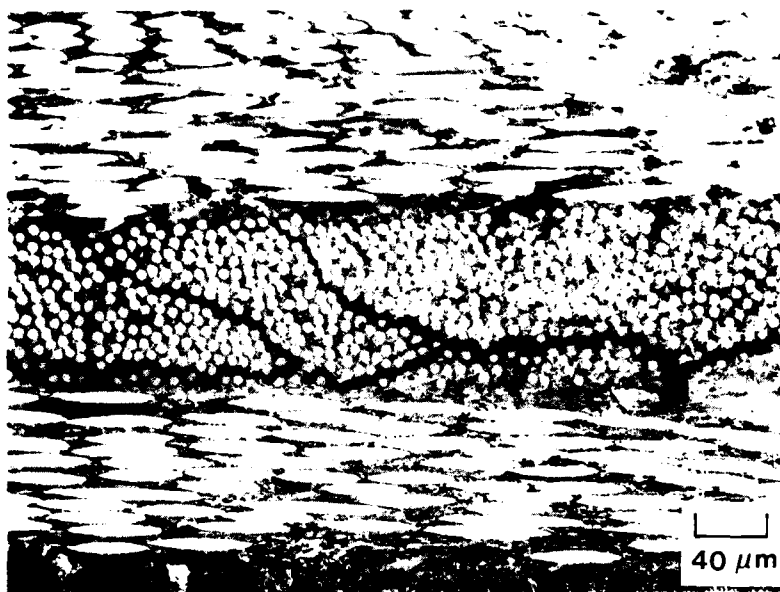
$$K_3 = 1.7 \times 10^{-6} \text{ dynes for PAA}$$

$$K_3 = 0.7 \times 10^{-6} \text{ dynes for MBBA.}$$

The elastic constant for bend for the mesophase, a discotic nematic liquid crystal, is about 10 times larger than the bend constant for rodlike liquid crystals. This difference may be related to the higher molecular weight and the disklike shape of the aromatic molecules. This is the first determination of one of the three elastic constants for bend, twist, and splay for the carbonaceous mesophase.

Alignment in Fiber Composite

The bulk mesophase, which is characteristic of the matrix between fiber bundles in a carbon-carbon composite, is aligned in the direction of the magnetic field. The resulting structure is the fibrous structure of Figure 33. The mesophase matrix within fiber bundles is not well aligned by a magnetic field due to the strong anchoring of the disklike molecules parallel to the fiber surfaces. Thus, for a composite, some degree of alignment of the matrix is expected. One of the primary failure modes of a bidirectional carbon-carbon composite is interlaminar shear. This shear fracturing occurs on planes parallel to the fiber laminate plies as shown in Figure 42. Since the easy cleavage direction for graphite is parallel to the layer planes, crack propagation perpendicular to the graphitic layers is difficult. This tough fracture direction is perpendicular to the axis of the fibrous structure



H-228

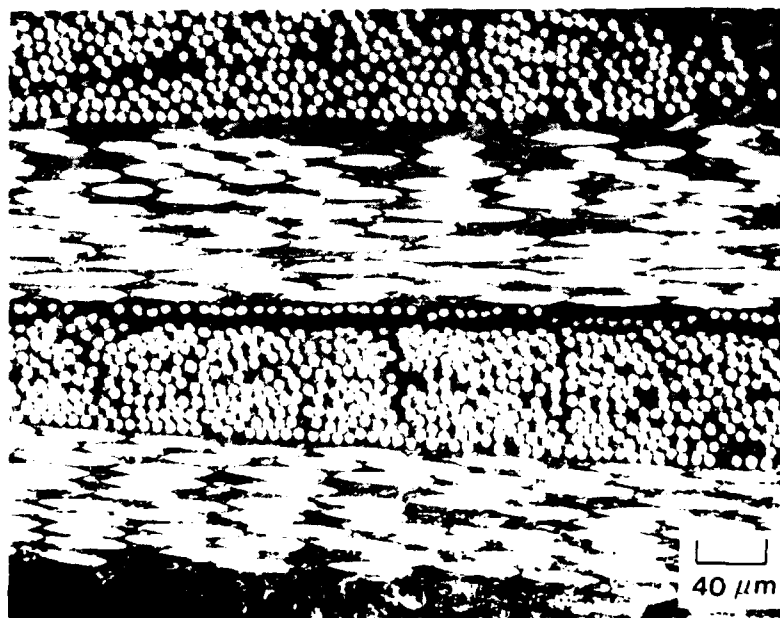


Figure 42. Optical micrographs of shear cracks in two-directional carbon-carbon composite

(Figure 33). Thus, if the composite matrix could be aligned with this fibrous structure perpendicular to the shear fracture plane, the composite may have improved shear properties. The magnetic field would be perpendicular to the fiber directions (Figure 43).

A graphite-fiber fabric (Fiberite F1041, T300 PAN, 8 harness satin weave, 23 x 24 ends/inch) was wrapped circumferentially inside the glass tubes and pyrolyzed with A240 pitch. The sample was held stationary in the magnetic field. On the diametrical plane containing the magnetic field, the fabric plies were perpendicular to the field as desired. On the diametrical plane perpendicular to the field, the plies were parallel to the field. This provided an alternate orientation for comparison. The basic structure of this bidirectional composite is shown in Figure 44. The two fiber bundle directions are perpendicular; some porosity is present and some porosity has been filled by the epoxy mounting medium.

Optical micrographs of the bidirectional composite are shown in Figures 45 through 47. The plane of section for these micrographs is perpendicular to the fabric plies and parallel to the magnetic field. In the top figure, the matrix between the fiber bundles is dark (in extinction), implying that the molecular layers are aligned and are perpendicular to the vertical polarizing direction. At the 45° rotation of the polarizers, this same aligned matrix is light, indicating it is now not perpendicular to the polarizers. These micrographs show that indeed the mesophase matrix between the fiber bundles is aligned perpendicular to the fabric plies.

The micrographs in Figures 48 and 49 show that the matrix is not similarly aligned when the magnetic field direction is parallel to the fabric plies. The structure of this matrix is relatively isotropic and contains

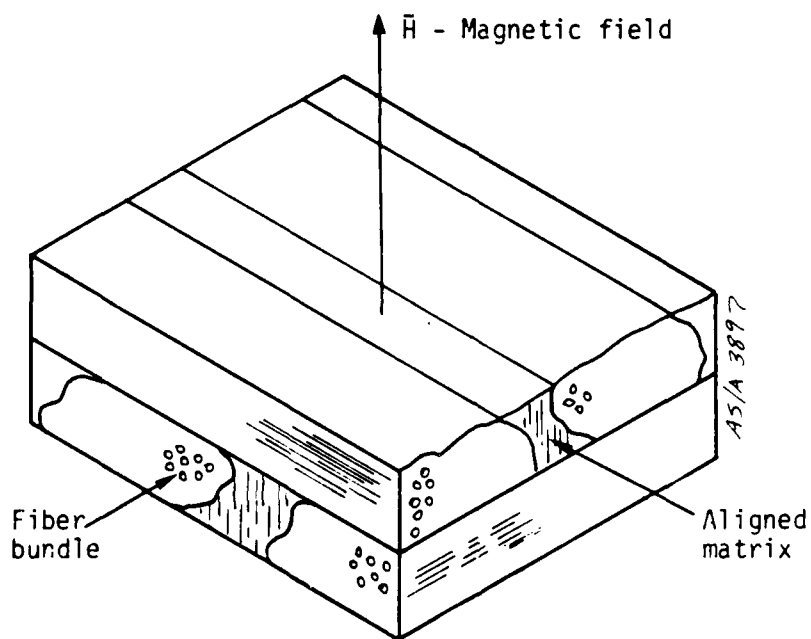


Figure 43. Schematic illustration of orientation of magnetic field and bidirectional composite

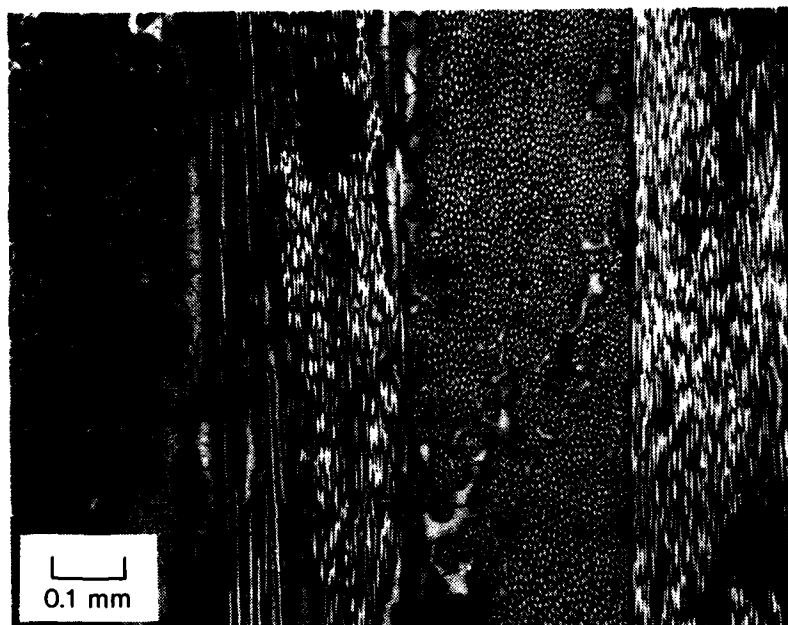


Figure 44. Structure of bidirectional composite; brightfield micrograph

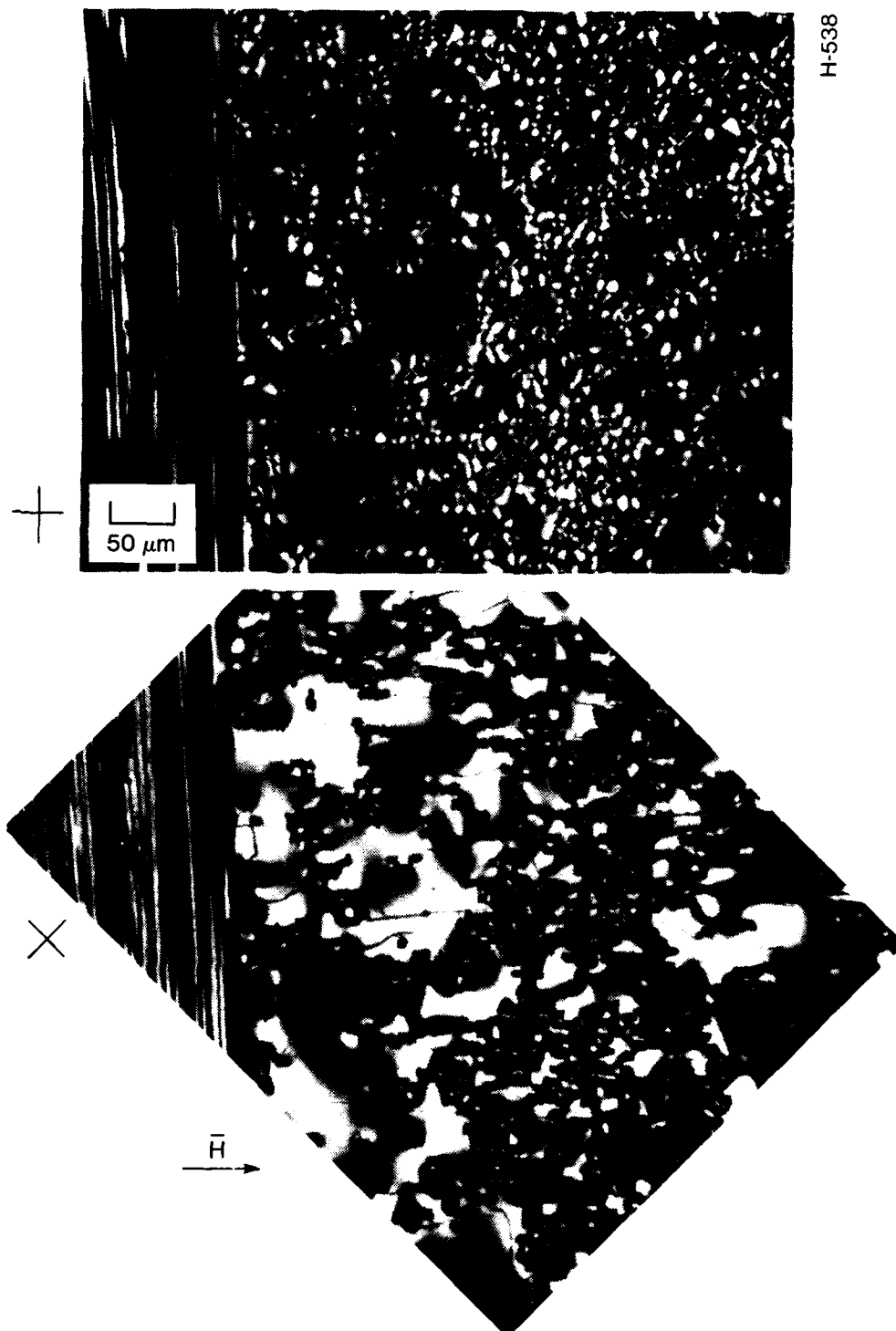


Figure 45. Optical micrographs of fiber composite pyrolyzed in magnetic field perpendicular to fabric plies: 5500 gauss, A240 pitch, 460°C, cross-polarized light micrographs

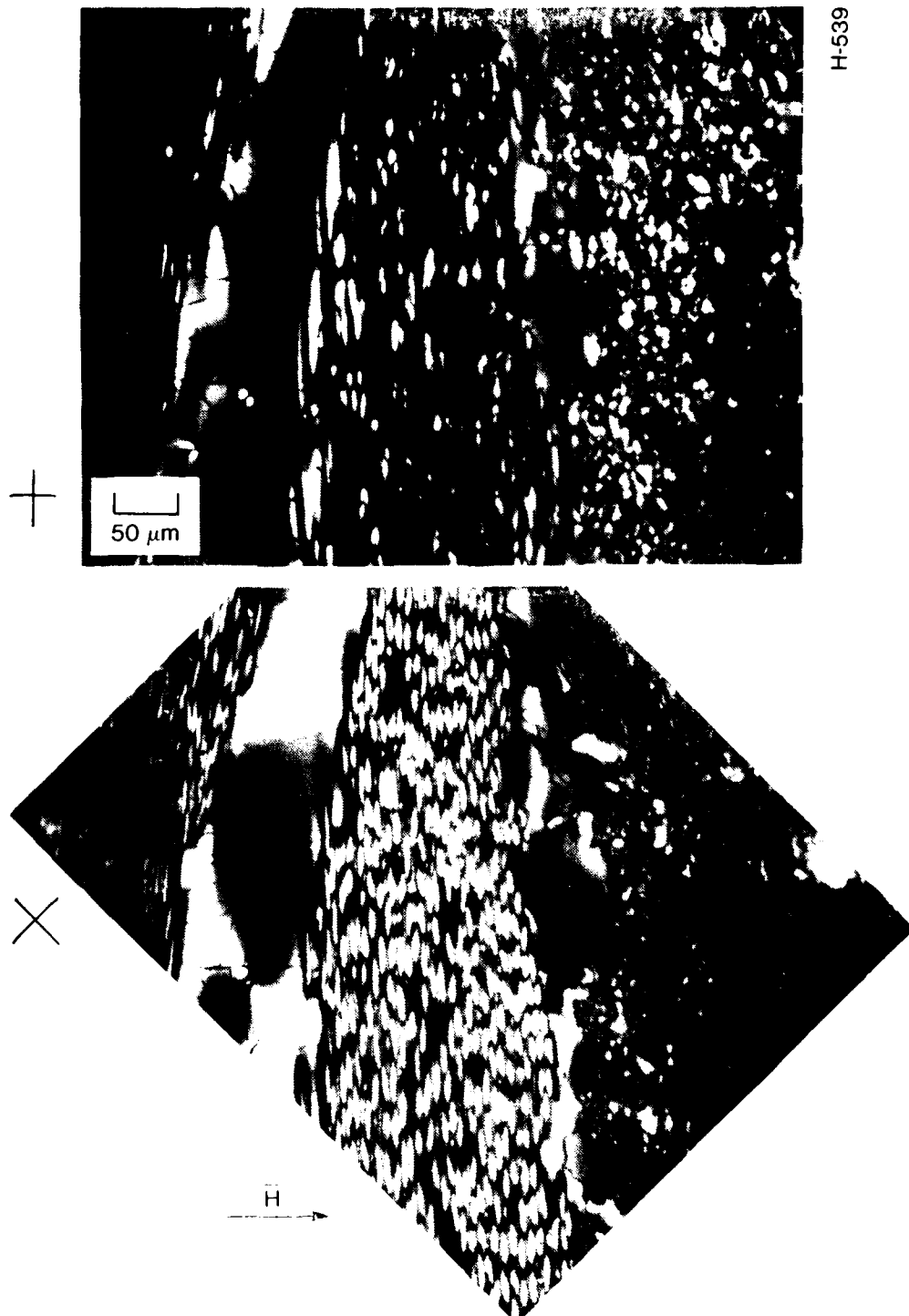


Figure 46. Micrographs of bidirectional composite perpendicular to magnetic field

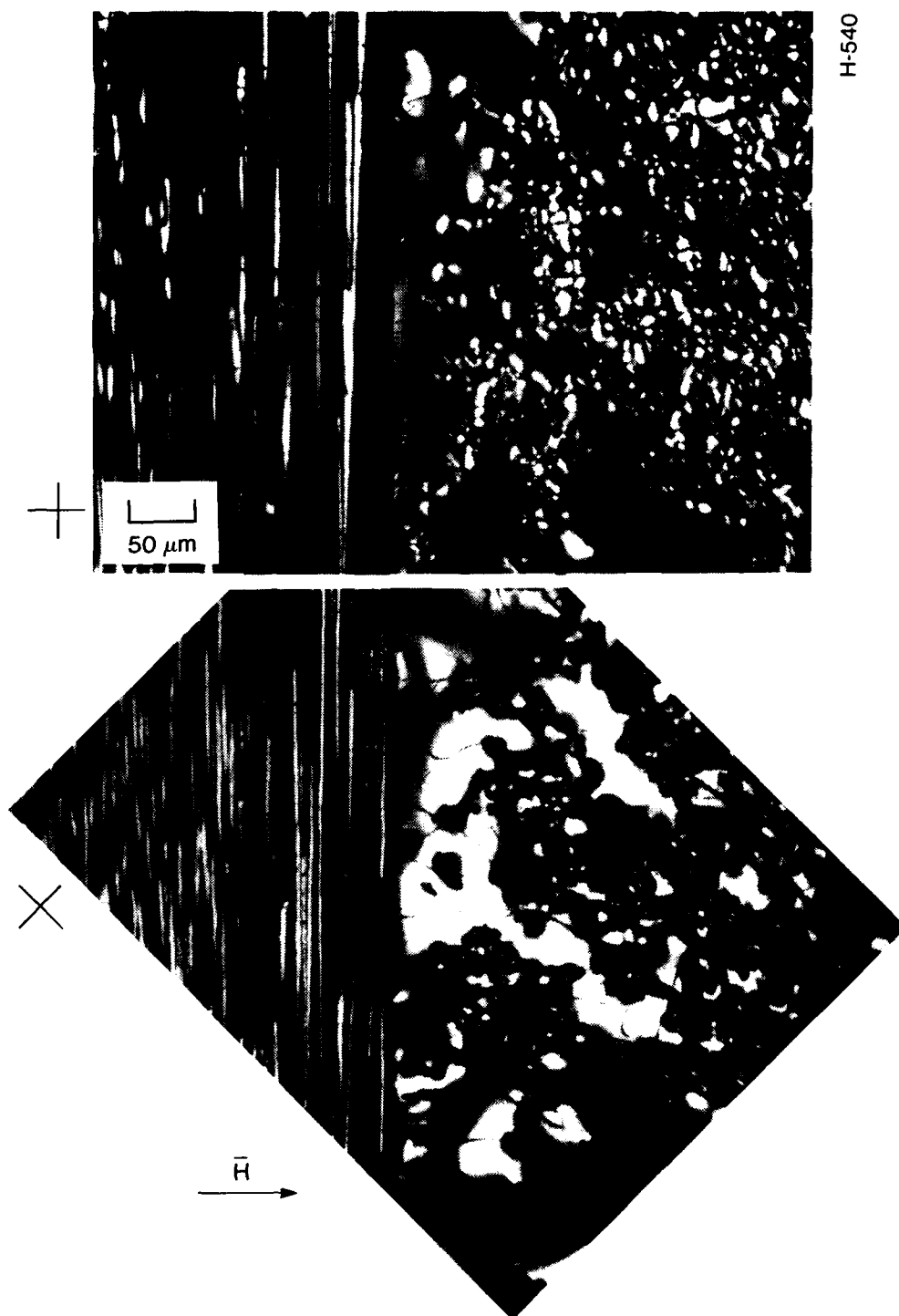
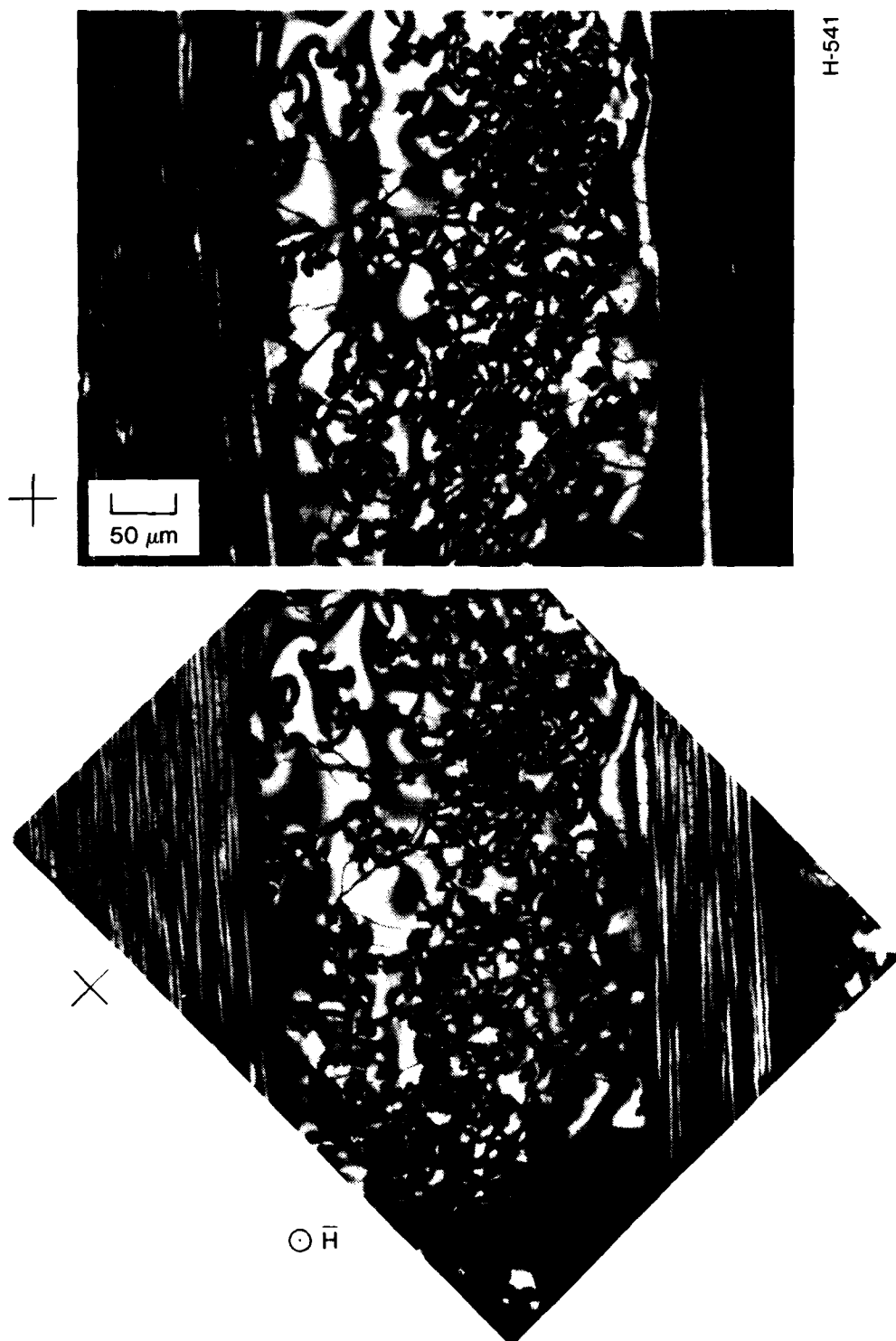


Figure 47. Micrographs of bidirectional composite perpendicular to magnetic field



H-541

Figure 48. Micrographs of bidirectional composite parallel to magnetic field

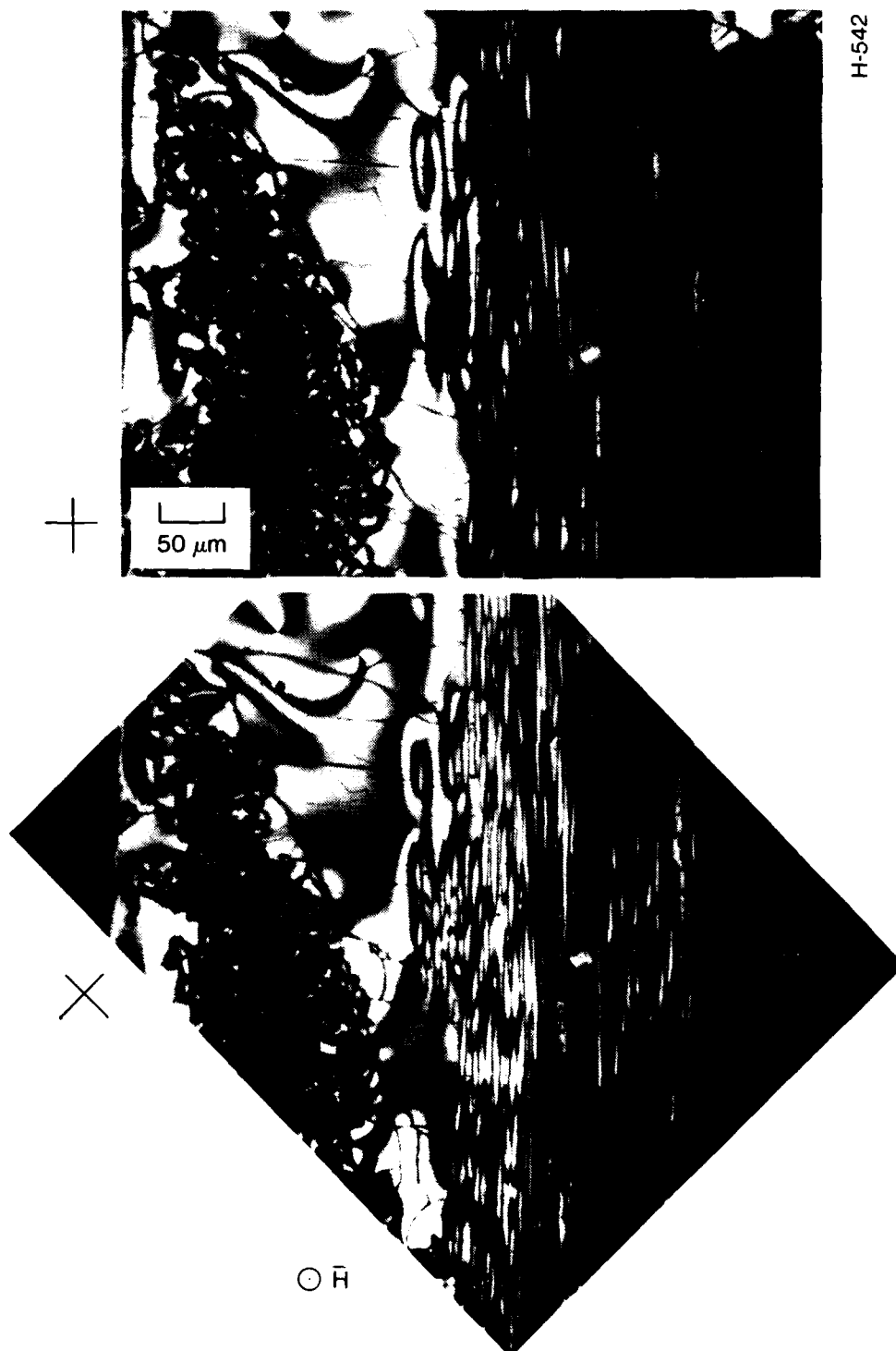


Figure 49. Micrographs of bidirectional composite parallel to magnetic field

disclinations. This is the structure of the fibrous microstructure as viewed on the cross section perpendicular to the fibrous axis.

These micrographs show that the magnetic field aligned the mesophase matrix between the fiber bundles perpendicular to the laminate fiber directions. The wedge disclinations in the fibrous microstructure of the matrix are aligned perpendicular to the fabric plies. This perpendicular alignment of the matrix should provide increased resistance to interlaminar shear fracture in this bidirectional composite. Further work on scaleup of this fabrication in a magnetic field and interlaminar shear testing is warranted.

PUBLICATION

The following technical publication has been prepared with support in part by this research program:

J. E. Zimmer and R. L. Weitz, Extended Abstracts, Carbone 84, International Carbon Conference, Bordeaux, France, July, 1984, p. 386: a paper entitled, "Three-Dimensional Disclination Arrays."

THREE-DIMENSIONAL DISCLINATION ARRAYS

J. Zimmer and R. Weitz

Acurex Corporation

555 Clyde Avenue, Mountain View, CA 94039

In a typical volume element of the carbonaceous mesophase, the disclination lines are oriented in many different directions. The lines may be curved or straight, and they may intersect each other. Identification and characterization of such a complex, three-dimensional array of disclinations is not simple. Although much information can be obtained from optical and scanning electron microscopy of a single metallographic plane of section, this analysis provides no information on the disclination arrays normal to this plane in the third direction. One technique to characterize the three-dimensional structure of the disclination arrays is to use mesophase microstructures with a high degree of preferred orientation¹. These include the fine fibrous structure of needle coke, the lamellar structure of bubble walls, and the aligned matrix in a graphite-fiber bundle. However, these specific microstructures are not always present in a carbon-carbon composite, especially in regions of the matrix between fiber bundles. Thus, another technique is needed to characterize the disclination arrays in matrix material that does not have a preferred orientation. This technique involves observation of a specific area on successive parallel planes of section.

Some features of the disclination arrays have been observed on a single plane of section. There tends to be an equal number of positive and negative disclinations such that the net rotation (strength) of a region of mesophase tends to zero. Disclinations of strength $S = \pm 1/2$ are more prominent than disclinations of strength $S = \pm 1$, since the energy of a disclination is related to the square of its strength. And along an extinction-contour line, the disclinations alternate sign. The observation of the three-dimensional arrays of disclinations was designed to determine whether the disclination lines are straight or curved, at what angles they intersect a typical single plane of section, and whether the disclinations intersect, and in what manner they intersect.

Experimental Procedure The technique of observing the same area on successive parallel planes of section required precise thickness measurements, skillful polishing, and careful procedures. The sample used was carbonaceous mesophase from Ashland A240 petroleum pitch heat treated at 400°C for 24 hr. This heat treatment produced mesophase with a coarse, undeformed microstructure with no specific preferred orientation. This mesophase microstructure is typical of the large matrix regions between fiber bundles in a carbon-carbon composite. Optical micrographs were taken after each plane of section of the same referenced area. Eight planes of section were observed; the total depth was 46 μm .

For each micrograph for each plane of section, a structural sketch was made to identify the underlying mesophase microstructure, including the disclinations. A series of micrographs at various rotations of the crossed polarizers were made and, with the use of an overlay, the orientation of the layers in the mesophase was sketched at each rotation. These structural sketches were then used to construct a three-dimensional picture of the disclination array. The core of each disclination was plotted, and the points connected to define the path of the disclination lines in-depth in the sample below the original plane of section.

Results The structural sketches constructed from the optical micrographs of the same area of mesophase are shown in Figure 1 for two of the eight successive parallel planes of section. This set of micrographs shows that there is some change in the disclination array. A three-dimensional sketch of the disclination array is presented in Figure 2. The points of intersection of each disclination line with each plane of section have been connected to illustrate the path of each disclination line. The lines generally traverse from the front face of the volume of mesophase to the back face (last plane of section). The apparent axial symmetry of these

disclinations suggest that these disclinations are wedge disclinations. Over the distance of the eight planes of section, none of the disclinations end abruptly. Topologically, a disclination line cannot end in the material.

Two significant features of the disclination array are evident. First, the disclination lines are curved. Over this small distance between the eight planes of section ($46\text{ }\mu\text{m}$), the amount of curvature is not great. For any plane of section, the disclinations are not generally normal to that plane. Second, and more interesting, is the evidence for the interaction of the disclinations. One disclination can separate into two disclinations, and two disclinations can join to one. The strength of such an interaction is conserved, that is, the total strength before the interaction equals the total strength after the interaction. For example, the first interaction consists of an $S = -1/2$ disclination branching to an $S = +1/2$, and an $S = -1$ disclination: $(S = -1/2) \rightarrow (S = +1/2) + (S = -1)$.

This is the first evidence for these disclination interactions in solid carbonaceous mesophase. This evidence was possible only by the technique of successive parallel planes of section. Similar disclination reactions have been observed by hot-stage microscopy on the free surface of the mesophase as a liquid.^{1,2} In this case, the disclinations interacted due to viscous flow of the mesophase. These same interactions are retained as the mesophase hardens to coke.

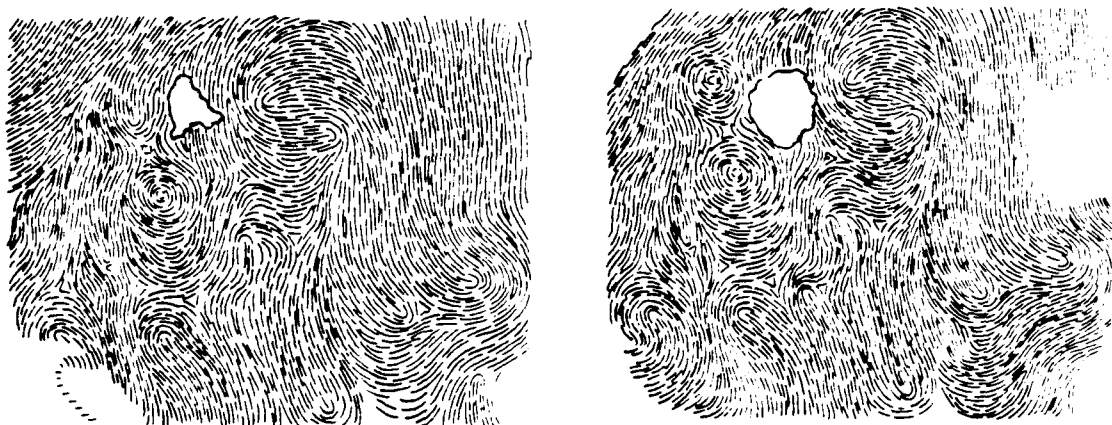


Figure 1. Structural sketch on fourth plane of section (left) and on fifth plane of section, $5\text{ }\mu\text{m}$ below fourth plane

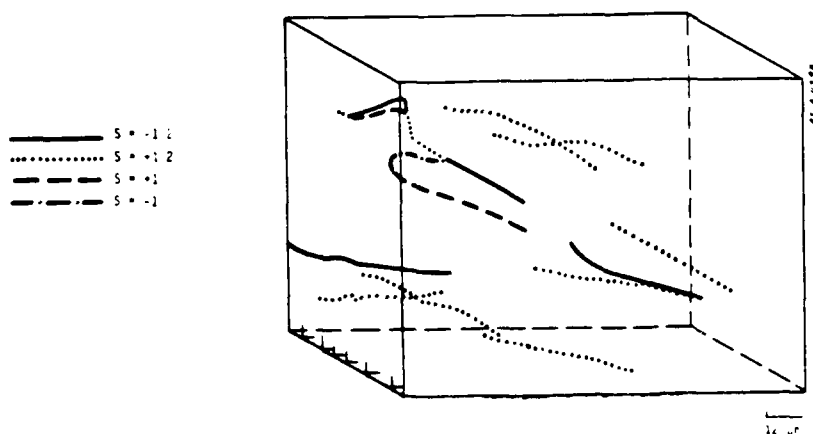


Figure 2. Sketch of the three-dimensional structure of the disclination array. The disclination lines begin on the front face (first plane of section) and end on the back face (eighth plane of section).

1. J. E. Zimmer and J. L. White, Advances in Liquid Crystals 5 (1982) 157
2. M. Buechler, C. B. Ng, and J. L. White, Extended Abstracts, 15th Conference on Carbon, (1981) 182.

REFERENCES

1. J. D. Brooks and G. H. Taylor, Chem. and Phys. of Carbon 4, 243 (1965).
2. J. L. White, Progr. in Solid State Chem. 9, 59 (1975).
3. J. L. White and J. E. Zimmer, Surface and Defect Properties of Solids 5, 16 (1976).
4. I. Mochida, K. Maeda, and K. Takeshita, Carbon 16, 459 (1978).
5. J. E. Zimmer and J. L. White, Advances in Liquid Crystals 5, 157 (1982).
6. J. D. Brooks and G. H. Taylor, Carbon 3, 185 (1965).
7. J. Dubois, C. Agace, and J. L. White, Metallography 3, 337 (1970).
8. J. E. Zimmer and R. L. Weitz, Technical Report TR-82-24/ATD, Acurex Corporation, September 1982.
9. J. E. Zimmer and R. L. Weitz, Technical Report TR-83-21/ATD, Acurex Corporation, September 1983.
10. L. S. Singer and R. T. Lewis, Extended Abstracts, 11th Conference on Carbon (1973) 207.
11. P. Delhaes, J. C. Rouillon, G. Fug, and L. S. Singer, Carbon 17 (1979) 435.
12. A. M. Levelut, F. Hardouin, H. Gasparoux, C. Destrade, and N. H. Tinh, J. Physique 42 (1981) 147.
13. P. G. de Gennes, The Physics of Liquid Crystals, Clarendon Press, Oxford, 1974.

END

FILMED

1-85

DTIC